1989

Optimal Design and Control of Distribution System Capacitors.

Nugroho Iwan Santoso
Louisiana State University and Agricultural & Mechanical College

Order Number 9025337

Optimal design and control of distribution system capacitors

Santoso, Nugroho Iwan, Ph.D.

The Louisiana State University and Agricultural and Mechanical Col., 1989

U·M·I
300 N. Zeeb Rd.
Ann Arbor, MI 48106

OPTIMAL DESIGN AND CONTROL OF DISTRIBUTION SYSTEM CAPACITORS

A Dissertation

Submitted to the Graduate Faculty of the
Louisiana State University and
Agricultural and Mechanical College
in partial fulfillment of the
requirements for the degree of
Doctor of Philosophy

in

The Department of Electrical and Computer Engineering

by
Nugroho Iwan Santoso
Engineer, Trisakti University, 1982
M.S., Louisiana State University, 1983
December 1989

ACKNOWLEDGMENTS

The author would like to express his gratitude and appreciation to Dr. Owen T. Tan for his friendship and guidance throughout the author's graduate program and his valuable assistance in the preparation of this dissertation. Appreciation is also expressed to Dr. Gili G. Richards for his assistance, Dr. Subhash C. Kak and Dr. Jerry L. Trahan of the Electrical & Computer Engineering Department, and Dr. James R. Dorroh of the Department of Mathematics for serving as members of the examining committee; recognition is also addressed to Dr. Powsiri Klinkachorn and Dr. Ali Mirbod who served as former members of the committee.

The financial assistance of the Electrical and Computer Engineering Department and the Electric Power Research Consortium sponsored by Louisiana Power and Light Co., Gulf States Utilities Co. and Central Louisiana Electric Co. is greatly acknowledged.

The author would like to express his sincere appreciation to his parents for their love and encouragement, and also to his friends, in particular R. K. Hartana and C. J. Yap, who have given constant support throughout his graduate and undergraduate studies.

TABLE OF CONTENTS

LIST OF TABLES

LIST OF FIGURES

ABSTRACT

The rapidly escalating costs of generation and transmission facilities as well as energy production have focussed attention on the need to optimize system capacity release and energy losses. The problem is generally solved by controlling the voltage or reactive power which also has a pivotal role within the distribution automatization schemes.

A review of reactive power compensators and methodologies in designing and controlling distribution capacitors is given. In the presence of voltage source harmonics, a local load reactive power compensation method, *cost-constrained power factor optimization using an LC compensator,* is discussed.

A new methodology based on a *piecewise method* for designing switchable capacitors installed on large distribution systems is described. Considered is the Var compensation problem concerning the optimal sizing and tap settings of capacitors installed on a radial distribution system such that for a given set of conforming load profiles, the energy and maximum power losses are minimized while the capacitor cost is taken into account. The algorithm is based on tearing the system into smaller subsystems, optimizing the individual subsystems and coordinating the subsystem solutions to yield the overall system optimization. Studies on a test system show the piecewise method to have satisfactory results as well as the significance of using appropriate load models.

The extent of benefit of shunt compensator application can be further maximized by providing an appropriate integrated control strategy for the compensators. An expert system using a *two-stage artificial neural control network* is proposed to control in real time the multitap capacitors installed on a distribution system for a nonconforming load

profile such that the system losses are minimized. The first stage of this control network has to predict the load profile from a set of prevailing input data obtained from direct measurements at certain buses as well as from the current tap positions of the capacitors. The second stage of the control network will select the optimal capacitor tap positions based on the load profile obtained in the first stage. The implementation of the control method to the test system shows the expert system to be computationally very efficient while having satisfactory results.

1. INTRODUCTION

In recent years, distribution automatization schemes in various stages of development and demonstration are beginning to take part in electric utility systems. Distribution automatization is seen by the electric utility industry as an integral part of the hierarchical system approach to the automatic generation control, substation or feeder monitoring and control, and load management needs of an electric utility system and also to system protection. The factors motivating distribution automatization, primarily economic in nature, are associated with the current emphasis on the expansion of existing facilities, ensured sufficient reliability, improved control, quality of service, and reduced operating cost [1].

It is generally acknowledged that the voltage/reactive power control function has a pivotal role within the distribution automatization schemes. The rapidly escalating costs of generation and transmission facilities as well as energy production have focussed attention on the need to minimize peak power demand and energy losses. Developments in distribution automatization through substation-based computer and feeder data acquisition systems allow a substantial reduction of system losses by real-time control of the reactive power flow and voltage on the distribution system.

Independent of the Var compensator configuration, shunt capacitors are widely used in distribution systems for reactive power compensation to achieve energy loss reduction, peak power reduction or system capacity release as well as improved voltage profile. The extent of these benefits depends on the number, location, size, type, and control strategy of the capacitors. These benefits are weighted against the cost of capacitor installation.

Several approaches such as nonlinear, linear, dynamic, integer programming,

and heuristics have been used to obtain an optimum solution for the capacitor allocation and control problem. The early approaches include works based on analytical methods by Neagle and Samson [2], Cook [3,4], Chang [5], and Schmill [6], and also a study based on dynamic programming developed by H. Duran [7]. These methodologies suffer from the lack of generality and consider an over-simplified model for the problem. Recently, growing needs of distribution automation have regenerated interest in the capacitor allocation and control problem. The resulting studies, which consider the problem in its more general form, can be classified into four approaches. The first one is the dynamic programming type approach by treating the capacitor sizes as discrete variables [8]. The second approach is to combine the conventional analytical methods with heuristics [9,10]. The third approach, pioneered by Grainger et al., is to formulate the problem as a nonlinear programming problem by treating the capacitor size and location as continuous variables [11-14]; the application of this approach which includes the voltage regulator problem is given in [1].

The last approach is mixed integer programming which combines the linear/nonlinear and integer programming in a certain arrangement. Baran and Wu [15,16] decomposed the problem into a "master problem" (for determining the number and location of the capacitors) which is solved by an integer programing method, and "base problems" (for obtaining the capacitor sizes) which are solved by nonlinear programming. Chiang et al. reformulated the problem in a more practical form and solved the discrete optimization problem using an annealing algorithm [17].

It is generally known, however, that a large system size presents a computationally very difficult, if not impossible, task for these optimal methods to converge, especially if the number of capacitors to be installed is not restricted. Conventional nonlinear optimization methods will introduce enormous computation times or divergence of the optimization iteration; dynamic programming methods are more suitable for feeders without laterals and sublaterals, and conventional integer programming methods (more known as

exhaustive combinatorial search) are not feasible for a large system because of the tremendous growth of the required computation time with system size.

Here, it is proposed to solve the capacitor problem by tearing (dividing) the overall system into smaller subsystems [18]. These subsystems are sequentially optimized by fixing the interaction variables shared by multiple subsystems before the optimization process of each subsystem is started. In the optimization formulation the effect of changing interaction variables on the other subsystems is incorporated. The optimum solution for each subproblem is much easier to achieve because of the smaller system size. The optimum solution for the overall system is obtained by coordinating the subsystem solutions. Herewith, the iteration variables on which the optimum solution of each subsystem has been based are updated, thus necessitating the optimization procedure to be performed repeatedly until convergence of the solution is obtained.

The capacitor problem considered here (optimal capacitor sizing problem) and solved by the piecewise method involves the determination of the optimal size and tap settings of the capacitors installed so that for a given set of "conforming" load profiles (loads vary in the same proportion of the total system load), the energy and peak power losses are minimized while the capacitor installation cost is taken into account. A solution methodology will decompose the sizing and tap setting problem into "base" problems which are concerned only with the optimization for a constant load level. The optimal number and location of the capacitors can be determined by any known method [1,15]; therefore, it will not be discussed. The algorithm allows individual loads to be represented by constant power sinks or constant impedances whereas the capacitors are invariably modeled as admittances.

Generally, power system harmonics are not considered here because of their minute effect on distribution system losses. However, their existence will lower the power factor [19] and introduce harmonic distortion of the distribution system voltages which may cause some undesired effects to the customers. A second order LC compensator is

proposed for optimizing the power factor of a local load while constraining the total cost of the compensator; its design algorithm is introduced and analyzed. Test studies on the compensator show that it can improve the power factor significantly while maintaining its cost equal to that of a pure capacitor compensator [20].

Another disadvantage of the conventional integrated design-control approach is the fact that most of the reactive power compensation methods for a distribution system are based on a load forecast where the individual loads change in the same proportion [1,8,9] of the total system load (conforming loads). The optimal capacitor control problem is then conveniently incorporated in the capacitor design and solved in its entirety. In practice, however, several load groups do not vary over the daily load cycle in the same manner as the rest of the system load so that a prevailing load profile cannot be readily predicted.

An accurate optimal capacitor control in real time can be obtained by modifying the algorithm of an optimal capacitor design bearing in mind that for the control part the capacitors are already available up to their maximum ratings. The main problem with this approach is the long computation time required as well as the impracticality of monitoring all loads continuously. The time consuming optimization procedure has to be performed for each load profile; similar load profiles will still require a separate optimization process. Therefore, it is desirable to develop a computationally efficient control strategy for the optimal capacitor settings which should be based on a limited number of on-line measurements only.

An expert system, a kind of artificial intelligence, is one of the most promising methods for fulfilling the requirements above. It has attracted widespread interest in recent years. The application of expert systems to power systems is still in an infant stage; however, much research has been made in this field. This includes fast power system voltage contingency analysis [21], automatic control of power systems in the restorative state [22], assisting decision making of reactive power/voltage control [23,24], intelligent load flow engine for power system planning [25], dynamic security assessment for electric

power systems [26], detection of incipient faults on power distribution feeders [27], and operational aid for restoration and loss reduction of distribution systems [28]. Most of those studies use rule-based expert systems; only two of them are based on an artificial neural network methodology [26,27].

A neural-net based expert system is proposed to solve the capacitor control problem by designing a specialized configuration of an artificial neural network which can learn from patterns encountered previously. The first stage of this control network has to predict the load profile from a set of the prevailing input data obtained from a few on-line measurements which include the active and reactive line power flows and the voltage magnitudes at certain buses as well as from the current tap positions of the capacitors. The second stage of the control network will select the optimal capacitor tap positions based on the load profile obtained in the first stage. The optimum control will not involve any iteration procedure, therefore, it is expected to be computationally very efficient.

2. VAR COMPENSATION METHODOLOGIES

The determination of reactive power compensation for power systems is mainly influenced by the design objective, period and parameter criteria or limitations. Other considerations include existing facilities and system reliability.

In general, the design objectives can be ranked from the most to the least important as follows [29]:

a. To provide steady state security or to maintain bus voltages within specified ranges.
b. To maintain dynamic system security or stability following a contingency.
c. To better utilize transmission facilities and maximize savings obtained from reactive power reduction.
d. To improve reactive reserve margins and generator power factor as well as to support energy interchange between systems.

The objective of the reactive power design for distribution systems is more concerned with the first and third objectives which can be combined into maximizing the savings obtained from reactive power reduction while maintaining the bus voltages within a specified range [1,30,31].

The parameter criteria of the reactive power design include

a. allowable bus voltage range which typically varies from 95% to 105% for normal operation, and 90 % to 110 % during contingency operation,
b. load level variations, typically 100, 85, 70, 50, and 30% during light load condition,
c. transformer type,
d. number, location, size, type and control strategy of the reactive power compensator,
e. contingencies considered (single, double, etc.), and
f. operating conditions considered.

The determination of the reactive-power compensator parameters is considered more complex and important than the other parameters which can be determined heuristically [29]. Therefore, in the following sections the different types and applications of Var compensators as well as the basic computational design methodologies will be briefly discussed.

2.1. Type of Var Compensator

Reactive power requirements of a power system are provided by several reactive power sources which include synchronous generators, synchronous condensors, static Var compensation devices, transmission lines and in-phase transformers. In certain situations, network reconfiguration can ease reactive power problems [32-33]. Reactive power compensators can be distinguished between passive and active compensators [34]. Passive compensators include compensators that apart from manual-switching, they are uncontrolled; this type of compensator is usually used only for surge-impedance and line-length compensation. Active compensators are usually capable of continuous variation and rapid response. A more general clasification of reactive power compensator devices includes static and dynamic compensators [29,34-36] which will be discribed briefly in the next sections. Emphasis is given to shunt compensators since they are the most wideiy used in today's power systems.

2.1.1. Static Var Compensator

Static refers to the fact that this compensator type has no moving parts. A static Var compensator (SVC) can be defined as any member of the reactive compensation system family composed of compensation elements, thyristor-switches, and the associated control system to provide rapid and refined adjustment of the system reactive power flow. The basic elements of static Var compensators include capacitors and reactors. Without the thyristor-switching components, these Var compensator elements are usually switched manually, in which case their response is relatively slow and not suitable for

fast compensation. A brief description of each such element follows.

Shunt Capacitors

Shunt capacitors are the most widely used compensator element in the power system industry. This type of compensator element has several advantages over the other compensators because it is economic, flexible (can be connected in series or parallel with any other shunt capacitor or reactor), expandable, transportable, reliable, and also it offers great control capability. Compensation provided by shunt capacitors is a function of the line voltage (voltage dependent).

Series Capacitors

The application of series capacitors is mainly for compensating the transmission line reactance, thereby raising system voltages, reducing line losses and enhancing system stability. However, series capacitors are not commonly used because of some disadvantages, i.e., they are exposed to high current all the time, causing resonance or ferroresonance, and subjected to high voltage in case of a short circuit.

Shunt Reactors

The application of shunt reactors includes for holding down the system bus voltage during periods when the system is lightly loaded and for reducing the magnitude of system switching surges. This type of compensator is generally found in systems with long lines or with a large number of underground cables.

Series Reactors

Other than for limiting or redistributing power flows on parallel lines, these Var compensators are hardly used.

Static Var compensators can provide continuous or discrete, instantaneous changes in the reactive power output and also independent phase control. The control circuit is generally connected through a coupling transformer or a tertiary transformer winding.

There are three basic control methods available for the compensator elements, i.e., manual, supervisory and automatic control in response to the bus voltage or loading. The drawbacks of static Var compensators include

a. application of solid state switches and their control will raise the cost of the shunt compensator itself by a factor of 2 or more; moreover, it will increase the system maintenance requirements,

b. some configurations create harmonics; therefore, additional filters are required.

A Var compensator may consist of one or several compensator components. Each compensator component can be constructed by combining a compensator element with a thyristor-based controller. In practice, there are three basic controlled components in building static Var compensators:

1. *Thyristor-controlled reactor (TCR).* The control element is composed of thyristor switches shown in Fig. 2.1 as two oppositely poled thyristors which conduct on alternate half cycles of the supply frequency. The current contains a small in-phase component due to the power loss in the reactor, which may be of the order of 0.5-2.0 % of the reactive power. S is a manual switch for energizing the compensator component.

The most common control principle is called phase control which can be explained as follows. Full conduction is obtained with a gating delay angle α of 90° (with respect to the voltage phase angle). Partial conduction is obtained with α between 90°and 180°. The effect of increasing the gating angle is to reduce the fundamental harmonic component I_1 of the current which can be found by Fourier analysis of the instantaneous current i:

$$i = \begin{cases} \frac{\sqrt{2}}{X_l} V (\cos \alpha - \cos \omega t), & \alpha < \omega t < \alpha + \sigma; \\ 0, & \alpha + \sigma \le \omega t \le \alpha + \pi, \end{cases}$$

$$I_1 = \frac{\sigma - \sin \sigma}{\pi X_l} V \qquad (2.1)$$

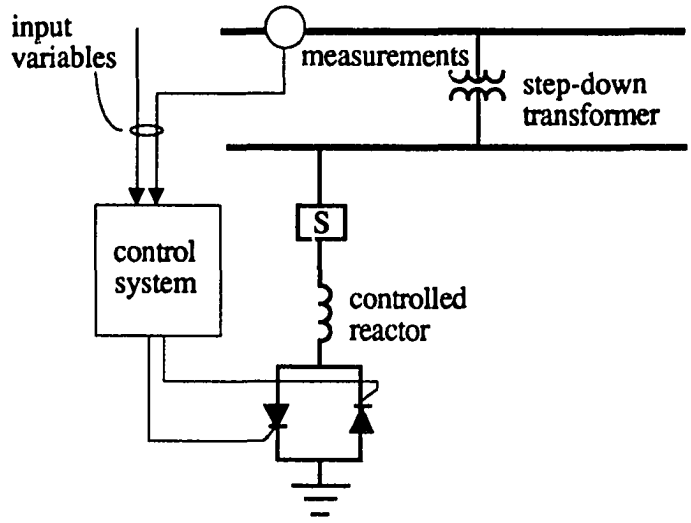

Fig. 2.1. Thyristor-controlled reactor

where

$$X_l = \omega L,$$

$$\omega = 2\pi f,$$

$$\sigma = 2(\pi - \alpha) \tag{2.2}$$

and

V : rms voltage across the compensator,

σ : conduction angle,

L : controlled reactor inductance.

Increasing α will have the same effect as increasing X_l which will reduce the current and losses in both the thyristor and reactor. However, the current waveform becomes less sinusoidal, therefore injecting higher harmonic current into the system. The n^{th} rms harmonic current component can be expressed as a function of α:

$$I_n = \frac{4V}{3X_l}\left[\frac{\sin(n+1)\alpha}{2(n+1)} + \frac{\sin(n-1)\alpha}{2(n-1)} - \cos\alpha\frac{\sin n\alpha}{n}\right], \quad n = 3,5,7,.. \tag{2.3}$$

Another variant of thyristor-controlled reactor is a thyristor-controlled transformer which can be realized by replacing the reactor with a transformer.

2. *Thyristor-switched capacitors (TSC).* As illustrated in Fig. 2.2, the capacitor susceptance is adjusted by controlling the number of parallel capacitors connected. With nc capacitors in parallel, each controlled by a thyristor-switch, the resultant susceptance can be equal to that of any combination of k, $k \in \{0, 1, 2, ...nc\}$, individual susceptances.

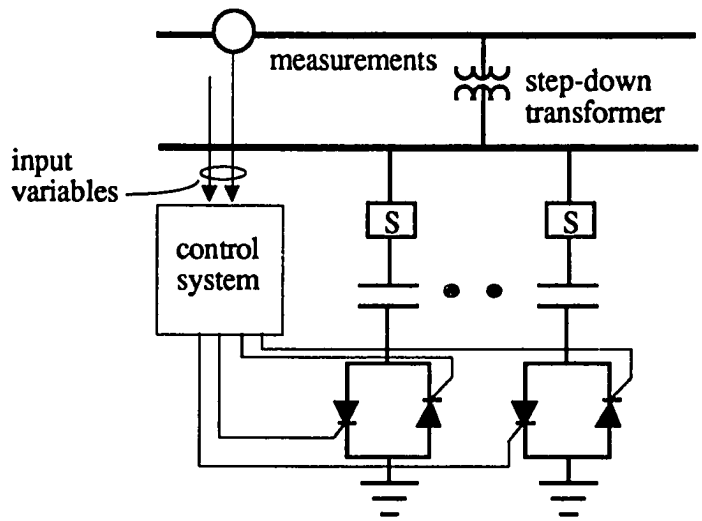

Fig. 2.2. Thyristor-switched capacitor

The resultant susceptance thus varies in a step size manner. In principle the steps can be made as small and as many as required by having a sufficient number of individually thyristor-switched capacitors.

3. *Saturated reactor (SR)*

This compensator type is mainly used for voltage stabilization. There are several basic control schemes available [34]; however, only one, the polyphase, harmonic-compensated, self-saturating reactor, has been developed and commonly used for voltage stabilization purposes (Fig. 2.3).

The operation principle is based on the magnetization characteristic of a magnetic cored inductor. The fundamental voltage across the saturable reactor is practically limited to its saturation voltage. As the voltage exceeds the saturation voltage, more reactive

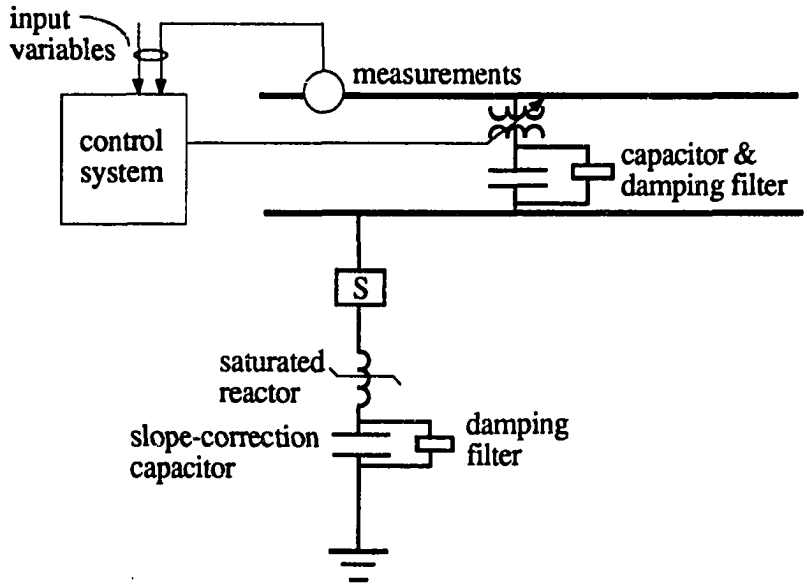

Fig. 2.3. Saturated reactor

current is drawn by the reactor which will cause higher voltage drop in the transmission line impedance. Therefore, the terminal voltage will be lowered to a value near the saturation voltage.

It is noted that all the above mentioned thyristor-controlled components are usually installed in combination with other manually-controlled or fixed components, i.e., fixed reactors (FR) and fixed capacitors (FC). The fixed capacitors are very often tuned with small reactors to harmonic frequencies to absorb harmonics generated by the thyristor-controlled components.

Static Var Compensation System (SVCS)

Conventional static Var compensation systems available in the market [29] include several combinations of the basic components described above, i.e., thyristor-controlled

reactors with fixed capacitors (TCR-FC), segmented TCR-FC which consists of several thyristor-controlled reactors connected in parallel with a set of fixed capacitors, thyristor-controlled transformers with fixed capacitors (TCT-FC), TCR/TCT with manually-switched capacitors, thyristor-switched capacitor with thyristor-controlled reactors (TSC-TCR), and a combination of saturable reactors and thyristor-switched capacitors (SR-TSC).

Apart from the conventional SVC systems there are several new configurations whose objective is to better provide the reactive power requirements of a power system. Two of the newest compensation schemes comprised of a super conducting coil (SC) and a forced commutated inverter (FCI) are still in their infant stage [29]. However, several designs based on those schemes have been developed and proven to have exceptional compensation characteristics. SC compensators provide lagging compensation with insignificant reactor losses. FCI can provide reactive power compensation as well as excellent harmonic compensation; however, it still has several undesired characteristics such as complexity, high cost and limited reactive power compensation capability.

2.1.2. Dynamic Var Compensator

Basically, there are only two kinds of dynamic Var sources, synchronous generators which are mainly designed for supplying real power and synchronous condensors which are specifically designed to generate reactive power only.

Synchronous Generators

In addition to supplying active power, synchronous generators are a major source of providing reactive power and reactive absorptive capability. They possess the dynamic ability to respond quickly to system perturbations and maintain voltages at desired levels; furthermore, they assert a strong stabilizing effect on system voltages. The ability to absorb reactive power is generally limited by the minimum limit of machine excitation, which is determined such as to provide adequate margin of safety for both the machine

thermal and steady state stability limits. Generally, synchronous generators are not suitable for compensating the total reactive power flowing in the system because of the following factors: (a) increased reactive capability carries a heavy economic penalty, and (b) because of its location, it is not effective to remedy low voltage problems along the distribution system. The unused reactive power output of the generator is often used as a source of reactive reserve to fulfill the requirements due to sudden disturbances only.

Synchronous Condensors

Practically synchronous condensor is a synchronous machine set up to generate reactive power only. It can be adjusted to deliver or absorb reactive power over a wide range by varying its excitation. While relatively more expensive than a static Var compensator, it offers some additional benefits such as continuous control, absorbtive and short-time overload capabilities, and better dynamic response characteristics over some static Var compensators.

Selecting the appropriate compensator requires a thorough analysis of the problem or requirement itself. This will yield a list of attributes which the candidate reactive power compensator must have in order to satisfy the requirements. Such attributes include

a. nature of reactive compensation, absorptive or productive,
b. magnitude,
c. extent of need, frequency and duration,
d. need for independent phase control,
e. impact of short circuit contribution, and
f. location on system with respect to load, generator and other Var devices, and system voltage level.

The most important attribute is the speed of response which in fact constitutes the main factor in classifying the reactive power requirements. An approximate guide for Var source applications [29] is listed in Appendix A.

2.2. Computation Methods

Numerous methods for solving the problem of optimal capacitor allocation have been presented in the literature [1-17,29,37]. This section reviews the basic methods that are relevant to the optimal allocation problem of reactive power in transmission and distribution systems.

General Optimization Problem

A general optimization problem can be stated as follows. Obtain

$$\mathbf{X} = [x_1, x_2, \ldots x_{nx}]_t \quad \text{which minimizes } f(\mathbf{X}) \tag{2.4}$$

subject to the constraints

$$ci_j(\mathbf{X}) \le 0, \qquad j = 1,2,\ldots nci, \tag{2.5}$$

$$ce_j(\mathbf{X}) = 0, \qquad j = 1,2,\ldots nce, \tag{2.6}$$

where

$\mathbf{X}$: nx dimensional control vector,

$f(\mathbf{X})$: objective function,

$ci_j(\mathbf{X})$: inequality constraint functions, and

$ce_j(\mathbf{X})$: equality constraint functions.

Basically, there are two kinds of optimum points, i.e., *local* or *relative* optimum and *global* or *absolute* optimum. A function $f(\mathbf{X})$ is said to have a local optimum at $\mathbf{X} = \mathbf{X}^*$ if $f(\mathbf{X}^*) \le$ or $\ge f(\mathbf{X}^* + h)$ for all values of h sufficiently close to zero. An optimum point $\mathbf{X} = \mathbf{X}^*$ is global if $f(\mathbf{X}^*) \le$ or $\ge f(\mathbf{X})$ for all $\mathbf{X}$ in the domain over which $f(\mathbf{X})$ is defined.

Optimization schemes can be differentiated between those which require partial derivatives of the objective function and those which do not. Two fundamental theorems for optimization algorithms which make use of the differential techniques are as follows.

Theorem 1 : Let a function $f(\mathbf{X})$ be defined in the interval $\mathbf{X}_a \leq \mathbf{X} \leq \mathbf{X}_b$ and have a relative optimum at $\mathbf{X} = \mathbf{X}^*$ where $\mathbf{X}_a \leq \mathbf{X}^* \leq \mathbf{X}_b$; if all partial derivatives of f(**X**), $f'(\mathbf{X}) = \partial f(\mathbf{X})/\partial x_i$, $i = 1, 2, \ldots nx$, exist as finite numbers at $\mathbf{X} = \mathbf{X}^*$, then $f'(\mathbf{X}^*) = 0$.

Theorem 2 : A stationary point $\mathbf{X}^*$ is an extreme point if it satisfies the following sufficient condition. The matrix of the second partial derivative of $f(\mathbf{X})$ (Hessian matrix) evaluated at $\mathbf{X}^*$ is positive definite when $\mathbf{X}^*$ is a minimum point, and negative definite when $\mathbf{X}^*$ is a maximum point; semidefinite cases include cases where the Hessian matrix may be neither positive nor negative definite at $\mathbf{X}^*$, e.g., the saddle point in a two dimensional optimization problem.

2.2.1. Analytical Methods

The analytical optimization methods are suitable for finding the optimum of continuous and differentiable functions. These methods make use of the techniques of differential calculus in locating the optimum points [2-6].

Based on the two fundamental optimization theorems stated earlier, several techniques have been developed for multivariable optimization with equality and/or inequality constraints [37]. The *direct substitution method* eliminates m variables from the objective function with the help of m equality constraints, the *method of constrained variation* eliminates m variations from the derivatives of the objective function, whereas the *method of Lagrange multipliers* eliminates the equality constraints by introducing one additional optimization variable to the problem for each constraint. Multivariable optimization with inequality constraints can be solved using the same method as with equality constraints; however, the inequality constraints have to be transformed into equality constraints by introducing non-negative slack variables and transforming the inequality constraints into *Kuhn Tucker conditions* which are necessary to be satisfied at a relative optimum point; however, these conditions are not sufficient to ensure a relative

optimum, except for a class of problems, called convex programming problems.

These analytical methods are intended for solving problems where the objective and constraint functions can be readily expressed in terms of the design variables. On the other hand, if the optimization problem involves an objective function and/or constraints which are not stated as explicit functions of the design variables or, which are too complicated to manipulate, these analytical methods cannot be applied. These problems can be solved by using numerical programming methods, e.g., nonlinear programming, linear programming, dynamic programming and integer or discrete programming methods.

2.2.2. Nonlinear Programming Techniques

An optimization problem is called a nonlinear programming (NLP) problem if any of the objective and constraint functions is nonlinear. This is the most general programming problem and all other programming problems can be considered as special cases of the NLP problem.

Numerical methods will be used for solving this type of problem. The basic philosophy of most of the numerical optimization methods is to produce a sequence of improved approximations to the optimum according to the following sequence.

1. Choose an initial point $\mathbf{X}_1$.
2. Find a direction vector $\Delta\mathbf{X}_i$ (initialize $i = 1$) which points in the general direction of the optimum point.
3. Find an appropriate iteration step λ_i for movement along the direction $\Delta\mathbf{X}_i$.
4. Obtain the next approximation point $\mathbf{X}_{i+1}$ as

$$\mathbf{X}_{i+1} = \mathbf{X}_i + \lambda_i \Delta\mathbf{X}_i \tag{2.7}$$

5. Check whether $\mathbf{X}_{i+1}$ is optimum. If yes, stop the procedure; otherwise, repeat steps 2-5.

From this procedure, it is noticed that the efficiency of an optimization algorithm depends

on the determination of λ_i and $\Delta \mathbf{X}_i$. Therefore, variations in the optimization methods will mainly be determined by the method of finding the iteration step λ_i and the direction vector $\Delta \mathbf{X}_i$.

Nonlinear programming methods are developed differently based on the nature of the problem [37]. There are methods developed for one-dimensional optimization problems, e.g., elimination techniques including unrestricted search, exhaustive search, dichotomous search, fibonacci method and golden section method [38], as well as interpolation methods which involve polynomial approximation for the given objective function. The assumption of unimodality is made in all the elimination techniques.

Other methods are developed to include multi-dimensional problems which could be constrained or unconstrained. Some relevant programming techniques include the steepest descent method and its modifications, i.e., Kuhn Tucker technique, penalty technique, Newton method and the augmented Lagrangian technique [29].

2.2.3. Other Numerical Programming Approaches

Linear Programming

Linear programming (LP) is an optimization method applicable to problems in which the objective function and all the constraints appear as linear functions of the design variables. The general linear programming problem can be stated in the following standard form. Optimize

$$f(\mathbf{X}) = \mathbf{C}_t \mathbf{X} \tag{2.8}$$

subject to the constraints

$$\mathbf{A}\,\mathbf{X} = \mathbf{B} \tag{2.9}$$

where $\mathbf{X}$ is the design variable vector ($n \times 1$ matrix), A, B and C are known constants ($n \times n$, $n \times 1$ and $n \times 1$ matrices respectively). Inequality constraints can always be transformed into equality constraints by adding slack variables. There are several linear programming methods, e.g., the simplex method and its modifications [37].

In linear programming methods, a nonlinear objective function, e.g., the objective function of Var allocation, is approximated by linear or piecewise linear function and the constraints are linearized around a given operating point. The resulting linear programming problem is then solved mainly by dual or primal simplex LP algorithms [29].

Dynamic Programming

Dynamic programming is a mathematical technique well suited for the optimization of multi-stage decision problems. It decomposes a multi-stage decision problem into a sequence of single stage decision problems. Thus an N-variable problem as a sequence of N single-variable problems is solved successively.

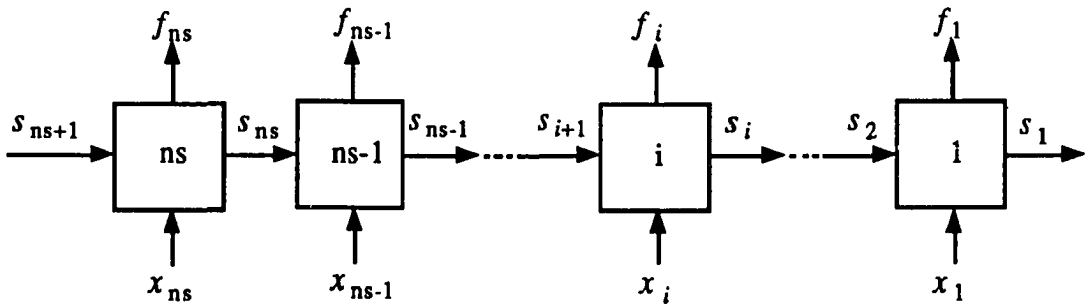

Fig. 2.4. Multistage decision process

A serial multistage decision process can be represented schematically as shown in Fig. 2.4. The objective of a multistage decision problem is to find $x_1, x_2, ...x_{ns}$, so as to optimize some function of the objective functions, $f(f_1, f_2, ..f_{ns})$, for the individual stages. Since the method functions as a decomposition technique, it requires the separability and monotonicity of the objective function. In order to have separability of the objective function, the objective function has to be represented as the composition of the individual objective functions; this composition can be additive or multiplicative.

A dynamic programming approach can be stated as follows. Find $x_1, x_2, ...x_{ns}$ which optimizes

$$f(x_1, x_2, \ldots x_{ns}) = \sum_{i=1}^{ns} f_i(s_{i+1}, x_i)$$

or

$$f(x_1, x_2, \ldots x_{ns}) = \prod_{i=1}^{ns} f_i(s_{i+1}, x_i) \tag{2.10}$$

and satisfies the design equations

$$s_i = fs_i(s_{i+1}, x_i), \qquad i = 1, 2, \ldots ns \tag{2.11}$$

This programming method makes use of the concept of suboptimization and optimality in solving the problem.

Principle of Optimality

This principle requires that x_i be selected so as to optimize f_i for a given s_{i+1}. This idea can be generalized and the i^{th} subproblem can be written as

$$f_i^*(s_{i+1}) = \underset{x_i}{\text{opt}} \; [f_i(x_i, s_{i+1}) + f_{i-1}^*(s_i)] \quad i = 2, 3, \ldots ns, \tag{2.12}$$

where $f_{i-1}^*(s_i)$ denotes the optimal value of the objective function corresponding to the last i -1 stages, and s_i is the input to stage i -1. Using the principle of optimality as stated in Eqn. (2.12), the original problem in Eqn. (2.10) has been decomposed into ns separate subproblems, each involving only one design variable.

Integer Programming

In all the numerical programming considered so far, each of the design variables is permitted to take on any real (or fractional) value. If an integer ('discrete' is more appropriate in many applications) solution is desired, it is possible to use any other techniques described previously and round off the optimum values of the design variables to the nearest integer/discrete values. However, in many cases it is very difficult to round off the solution without violating any of the constraints and/or causing non-optimal conditions. All these difficulties can be avoided if the optimization problem is posed

and solved as an integer programming problem.

When all the variables are constrained to take on only integer/discrete values in an optimization problem, it is called an integer programming problem: when only some variables are restricted to take on integer values, the optimization problem is called a *mixed-integer programming* problem.

Two of the most popular methods for solving linear integer/mixed-integer programming problems are the *cutting plane* algorithm of Gomory and the *branch-and-bound* algorithm [37]. A more efficient algorithm has also been developed by Balas [37] for a special case of integer programming problem where the optimization variables only take on values of either zero or one (or any other twofold values). Nonlinear integer programming problems are usually solved by the *generalized penalty function* method [37].

2.2.4. Gradient Methods

These methods require the partial derivative of the objective function f with respect to each of the n variables which are collectively called the gradient of the function and is denoted by ∇f:

$$\nabla f = \begin{bmatrix} \partial f / \partial x_1 \\ \partial f / \partial x_2 \\ . \\ . \\ \partial f / \partial x_{nx} \end{bmatrix} \tag{2.13}$$

Gradient methods are based on the fact that if the iteration path follows the gradient direction from any point in the n-dimensional space, the function increases or decreases at the fastest rate. However, the direction of the steepest ascent or descent is a local property and not a global one.

Steepest Descent Technique

This method applies the same nonlinear optimization sequence explained in section

2.2.2. The iteration starts from an initial point $\mathbf{X}_1$ and iteratively moves towards the optimum point according to

$$\mathbf{X}_{i+1} = \mathbf{X}_i \pm \lambda_i^* \nabla f_i. \tag{2.14}$$

The addition or subtraction sign refers to the maximization or minimization process respectively. λ_i^* is the optimal iteration step length for the search direction vector ∇f_i and is obtained by minimizing $f(\mathbf{X}_i \pm \lambda_i \nabla f_i)$ with respect to λ_i.

Several convergence criteria can be used to terminate the iterative optimization process, i.e.,

$$\left| \frac{f(\mathbf{X}_{i+1}) - f(\mathbf{X}_i)}{f(\mathbf{X}_i)} \right| \leq \varepsilon,$$

$$\left| \frac{\partial f}{\partial x_i} \right| \leq \varepsilon$$

or

$$|\mathbf{X}_{i+1} - \mathbf{X}_i| \leq \varepsilon, \tag{2.15}$$

where ε is the stopping tolerance value which is a predetermined small positive number. As a rule, it is difficult to find λ_i^*; therefore, a constant or gradually decreasing value for the iteration step may be attempted.

2.3. Var Compensation for Systems with Harmonic Sources

Nonlinear loads in power systems inherently produce harmonic voltages and currents. From the utility customer's point of view, harmonics can be classified as those generated by the customer load itself (such as static converters, electric machines, arc funaces and arc welders, gaseous discharge lighting, and static Var compensators) , which should be compensated locally (*local compensation*); and those which are caused by utilities' power components (medium and high power static converters, saturated transformers and generators) and other utility customers whose nonlinear loads have

created voltage distortions at a common voltage bus. A distorted bus voltage causes harmonic currents to flow in the linear compensated loads, particularly if series resonance occurs between the Thevenin source impedance and the compensated load. A customer with such a linear load needs to minimize the harmonic line current while simultaneously using a compensator to maintain a high power factor [20].

From the utility company's point of view, it is important to keep the harmonic contents below a certain maximum level to satisfy the quality standards, and also to prevent unwanted effects on the power system components. This will lead to an *overall compensation* whose objective is to lower the overall *total harmonic distortion* (THD) level regardless of the origin of the harmonic. This should be done in addition to voltage profile improvement and energy loss reduction.

2.3.1. Harmonic Effects

Harmonics are undesirable because of their negative effects on the utilities' power components and customers' power devices. It is generally known that harmonics may affect any of the four categories [39]:

a. power components, i.e., capacitor banks, transformers, electric machines and transmission-distribution lines,
b. instrumentation, e.g., watthour meters, ripple control systems and power system protection,
c. overall system power factor, and
d. communication systems.

Harmonic Effects on Capacitor Banks

The harmonic effect on capacitor banks is of particular interest for the design and control of those capacitors; a more detailed description on this subject is thought to be beneficial.

There are two main negative effects of using capacitor banks in the presence of

harmonics: additional capacitor power losses and possible capacitor destruction due to overvoltage as well as overvoltage (and also unacceptable THD level) at some buses caused by harmonic resonance. The first effect can be reasoned as follows. Capacitor impedance decreases with higher frequency. For this reason, capacitor banks act as *sinks* for harmonic currents. In a system with distributed harmonic sources, the harmonics will flow through the capacitor banks, and may result in fuse-blowing or capacitor failure. The increased total power loss in capacitor banks in the presence of harmonics is expressed by

$$P_{loss} = \sum_{n \in C_h} C \tan \delta_n \, \omega_n V_n^2 \qquad (2.16)$$

where $\tan \delta_n$ is the capacitor loss factor for the n^{th} harmonic, ω_n is the angular harmonic frequency, V_n is the rms value of the n^{th} harmonic voltage and C_h is the set of existing harmonic orders in the system.

Secondly, capacitor banks may cause a resonant circuit with the rest of the system impedance at a frequency near a harmonic frequency [40-42]. This can result in overvoltages and excessive currents often leading to their destruction. The THD will also be high, which most probably will exceed the allowable THD level. Moreover, the higher total reactive power including the fundamental and harmonics will require a capacitor with a higher rating, which means a more expensive capacitor.

2.3.2. Approach Overview

Local Compensation

Several methods have been proposed for optimal power factor correction at linear loads where source harmonics cause a problem. Complete compensation of the reactive voltamperes, which is defined as the product of rms voltage and the rms value of reactive current components, can be accomplished by applying a single port shunt compensator generally consisting of N ($2N$ - 1) reactance elements [20], where N is the number of harmonics present in the source voltage. For some particular loads, the number of

reactance elements may be less than that given by the formula [43].

If it is desired that compensator complexity be restricted, then the reactive voltamperes can only be partially compensated. Shephard and Zakikhani [44], and Chu [38] used a shunt capacitor to maximize the power factor. A second-order shunt compensator in the form of a series *LC* branch was shown by Czarnecki [45] to achieve a higher power factor than that achieved with pure capacitive compensation. However, the procedure given for the optimization would lead to an infinite number of *LC* combinations. Even if power factor were optimized with respect to both reactance elements, the resulting equations might not have a solution. In all these approaches to achieving the maximum possible power factor, the effect of harmonic voltages and currents on capacitor and inductor cost has been ignored. A cost constrained *LC* compensator will be discussed in the next section.

Overall Compensation

There are several approaches to eliminate or reduce the effect of harmonics on capacitors. In [46], an algorithm for optimizing shunt capacitor sizes on radial distribution lines with nonsinusoidal substation voltages such that the rms voltages and their corresponding total harmonic distortion lie within prescribed values is presented. The problem is formulated as a combinatorial optimization problem with inequality constraints. The optimal solution is determined by a heuristic numerical algorithm that is based on the method of local variation. However, it is implied that this approach only provides a cure for high harmonic levels caused by resonance. Therefore, it is possible that the algorithm will fail in finding an optimal solution when the high THD level is caused by an excessive amount of current harmonic injection.

Another approach is to provide an additional overall compensator-filter to detune the capacitor and at the same time reduce the harmonic contents in the system by drawing the harmonics into the ground [47].

2.3.3. Cost-Constrained *LC* Compensator

By constraining the compensator cost, it is shown [20] that the power factor can be maximized by using an *LC* compensator, and that this compensator cost may actually be lower than that for purely capacitive compensation at the same power factor.

Physical Interpretation

To illustrate the optimization process (summarized in Appendix B) and search regions to be used, a three-dimensional plot of the power factor as function of X_L and X_C is shown in Fig. 2.5, which is based on the parameter data given in Ref. 20 for two different compensator costs. Generally, a family of infinitely thin power factor ridges with the cost as parameter can be identified in each of the zones as shown in the figure, which are separated from each other by series-resonance lines.

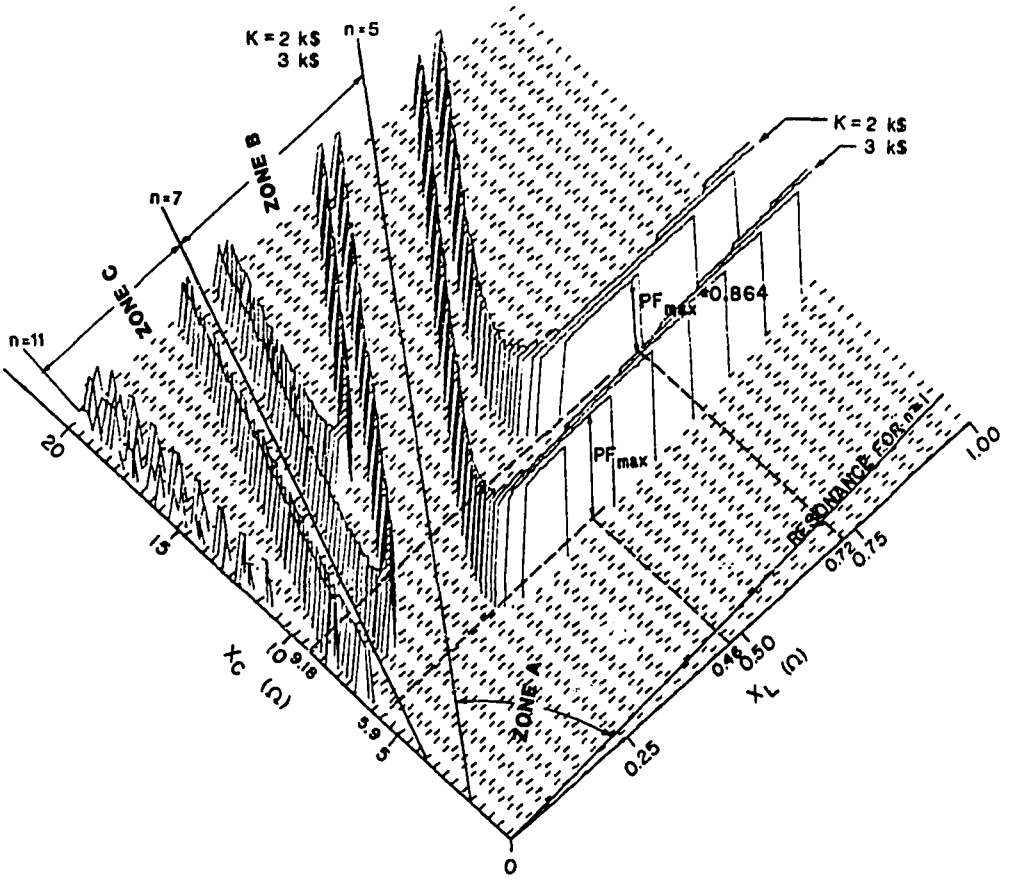

Fig. 2.5. Cost-constrained power factor as function of X_L and X_C

A series-resonance line represents all possible combinations of X_L and X_C values which result in series resonance between the Thevenin impedance and compensated load at a source harmonic frequency. Under these conditions, the power factor will reach a minimum. It is evident that the number of series-resonance lines will depend on the number of harmonics present in the Thevenin source.

Note that a ridge running nearly parallel to a resonance line implies that the corresponding *LC* combinations will approximately offer a constant impedance to the harmonic whose order corresponds to the resonance line. Where a power factor ridge reaches a maximum, a compromise has been achieved between the fundamental frequency compensation and the presence of harmonic currents which reduce power factor, such that the resultant line current is a minimum for the given cost. By comparing the zonal ridge maxima for a given cost, the global maximum power factor can be obtained. In the example considered, the global maximum power factors were found in the zone enclosed by the lowest order resonance lines. For K= 3 k$ and 2 k$, they are, respectively, 0.937 and 0.864, and are located at $X_L^* = 0.46\ \Omega$, $X_C^* = 5.9\ \Omega$, and $X_L^* = 0.72\ \Omega$, $X_C^* = 9.18\ \Omega$.

It is noted that the global maximum of the power factor is not necessarily located in the zone enclosed by the lowest order series-resonance lines. A different harmonic content in the voltage source may result in a global maximum of the power factor in a zone enclosed by higher order resonance lines.

3. OPTIMAL DESIGN OF SWITCHABLE DISTRIBUTION CAPACITORS BY PIECEWISE METHOD

The problem of large system size in the optimal design of switchable capacitors installed on a radial distribution system will be solved by a piecewise method. The algorithm is based on tearing the system into smaller *subsystems*, optimizing the individual subsystems, and coordinating the subsystem solutions to yield the overall system optimization [48]. The solution approach will be described after the optimization problem is formulated. The solution algorithm will be validated on a realistic test system for two types, constant power and constant impedance, of distribution system loads.

3.1. Introduction to Piecewise Methods

The basic idea of a piecewise method is to solve a problem for a large system by tearing the system apart into smaller subsystems or parts. The problem for each of the individual parts is solved, then by combining and modifying the solutions of the parts, the solution to the problem for the untorn system is obtained [18]. The result of the procedure is identical to one that would have been obtained if the system had not been torn apart. One obvious advantage of the piecewise method is that large system problems can be solved efficiently because of the much smaller size of the subsystems. Another is the possible application of multiprocessor/multicomputer parallel computation scheme which will further reduce the overall computation time. Also note that piecewise methods allow different solution procedures and iteration algorithms for the different subsystems. Applications of piecewise methods to power systems include multiarea economic dispatch, multilevel generation control of power pools and superpools, tie modeling, inter-area matrix modeling, and static and dynamic system analysis [49,50].

Two of the most common piecewise methods will be described in this section [18,50]. The first one is called the boundary iteration method which is conceptually a simple approach. The second one, a more sophisticated approach, is called diakoptics. There is mathematically no limit to the number of subsystems that can be considered, nor to their individual size. However, in practice, there is a restriction on how to choose the lines of tear and the maximum number of buses in each subsystem. In the targeted application the torn subsystems must be radially attached at the common bus (although the diakoptics theory applies to the more general case of multiple common buses [18]) and the maximum number of buses in each subsystem must be small enough so that the original problem does not reoccur.

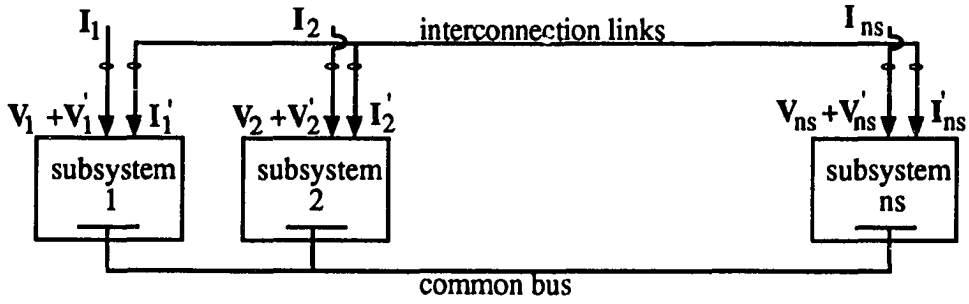

Fig. 3.1. Overall system torn into subsystems

The assumptions made include:

a. No mutual coupling exists between branches that are within different subsystems; however, mutual coupling between branches within a subsystem and also between links interconnecting the subsystems are allowed.

b. Series voltage sources are eliminated except those in the interconnecting branches.

Tearing Level

Both methods (boundary iterative algorithm and diakoptics) will apply the same tearing procedure which can be described as follows.

Step 1. Tear the network into ns subsystems and one set of links so as to facilitate the computation in each subsystem, e.g., each subsystem has no more than nb^{max} buses (nb^{max}=7 is used later for a test system). The primitive impedance of the torn network can be represented by

$$\mathbf{i}_b = \mathbf{y}_b \cdot \mathbf{v}_b \tag{3.1}$$

or

$$\begin{bmatrix} \mathbf{i}_{b1} \\ \mathbf{i}_{b2} \\ \cdot \\ \cdot \\ \mathbf{i}_{bns} \\ \mathbf{i}_l \end{bmatrix} = \begin{bmatrix} \mathbf{y}_1 & & & & & \\ & \mathbf{y}_2 & & & & \\ & & \cdot & & & \\ & & & \cdot & & \\ & & & & \mathbf{y}_{ns} & \\ & & & & & \mathbf{y}_{ll} \end{bmatrix} \begin{bmatrix} \mathbf{v}_{b1} \\ \mathbf{v}_{b2} \\ \cdot \\ \cdot \\ \mathbf{v}_{bns} \\ \mathbf{v}_l \end{bmatrix} \tag{3.2}$$

where

$\mathbf{v}_{bi}$: branch voltage vector of subsystem i,

$\mathbf{v}_l$: branch voltage vector of the set of links,

$\mathbf{i}_{bi}$: branch current vector of subsystem i,

$\mathbf{i}_l$: link current vector,

$\mathbf{y}_i$: primitive admittance matrix of subsystem i,

$\mathbf{y}_{ll}$: diagonal admittance matrix of link branches, and

ns : number of subsystems.

Step 2: Construct the bus impedance matrices of the individual subsystems either by the Z_{BUS} *building algorithm* or by inversion of $\mathbf{Y}_{BUS}$ [51], and write Eqn. (3.2) in the following form:

$$\begin{bmatrix} \mathbf{V}_T \\ \mathbf{v}_l \end{bmatrix} = \begin{bmatrix} \mathbf{Z}_{TT} & 0 \\ 0 & \mathbf{Z}_{ll} \end{bmatrix} \begin{bmatrix} \mathbf{I}_T + \mathbf{I}_T' \\ \mathbf{i}_l \end{bmatrix} \tag{3.3}$$

with

$$\mathbf{V}_T = [\mathbf{V}_1\ \mathbf{V}_2 \ldots \mathbf{V}_{ns}]_t$$
$$\mathbf{I}_T = [\mathbf{I}_1\ \mathbf{I}_2 \ldots \mathbf{I}_{ns}]_t$$
$$\mathbf{I}'_T = [\mathbf{I}'_1\ \mathbf{I}'_2 \ldots \mathbf{I}'_{ns}]_t$$
$$\mathbf{Z}_{TT} = \mathbf{diag}(\mathbf{Z}_1, \mathbf{Z}_2, \ldots \mathbf{Z}_{ns}) \tag{3.4}$$

where

$\mathbf{V}_i$ = bus voltage vector of subsystem i,

$\mathbf{I}_i$ = bus current vector of subsystem i,

$\mathbf{I}'_i$ = link current vector injected into subsystem i,

$\mathbf{Z}_i$ = bus impedance matrix of subsystem i, and

$\mathbf{Z}_{ll}$ = diagonal impedance matrix of set of links.

The overall subsystem bus voltages can then be expressed as

$$\mathbf{V}_T = \mathbf{Z}_{TT} \cdot \mathbf{I}_T + \mathbf{Z}_{TT} \cdot \mathbf{I}'_T \tag{3.5}$$

Note that $\mathbf{I}_T$ represents the externally applied currents, i.e., source and/or equivalent injected currents, and $\mathbf{I}'_T$ is the closed-path current vector due to the interconnection representing the contribution of the set of link currents $\mathbf{i}_l$.

Interconnecting Level

In the boundary iteration algorithm, $\mathbf{I}'_T$ is determined by an iterative method. Using the diakoptic method, $\mathbf{I}'_T$ is found non-iteratively for a linear case by employing orthogonal network theory. The advantage of the boundary iteration method is its simplicity.

3.1.1. Boundary Iteration Algorithm

This method requires an iterative procedure among the subsystem solutions even for linear cases. In nonlinear cases, the interconnection of the subsystems is expected to

contribute to increasing the number of iterations required to a degree depending on the relative effect of the interconnection ties.

By knowing the external injection currents $\mathbf{I}_T$ and equating the closed path currents $\mathbf{I}_T^{'}$ to 0, the initial estimates of the subsystem voltages $\mathbf{V}_T$ are computed by using Eqn (3.3); then the voltages across the link branches $\mathbf{v}_l$ are also found, and in turn the link currents $\mathbf{i}_l$ and the new closed path currents $\mathbf{I}_T^{'}$ are obtained. With $\mathbf{I}_T$ and $\mathbf{I}_T^{'}$ ascertained, the new terminal voltages in the subsystems $\mathbf{V}_T$ are determined.

With the new bus voltages at the interconnections known, corrections in $\mathbf{I}_T^{'}$ can be made and the procedure is repeated until the differences between two successive values of $\mathbf{i}_l$ and/or $\mathbf{V}_T$ are relatively small.

3.1.2. Diakoptics

Diakoptics provides a closed form solution and does not require cyclic calculation for the linear case. The effect of interconnection by diakoptics can be described as follows.

Step 1. Construct the link-bus incidence matrix C_l^T which transforms the link vector $\mathbf{i}_l$ into the closed-path current vector $\mathbf{I}_T^{'}$:

$$\mathbf{i}_l = C_l^T \, \mathbf{I}_T^{'} \tag{3.6}$$

Step 2. Compute the transformed impedance

$$\mathbf{Z}_{TT}^{'} = \left[C_l^T\right]_t \mathbf{Z}_{TT} \; C_l^T + \mathbf{Z}_{ll} \tag{3.7}$$

Step 3. The set of link currents is obtained from

$$\mathbf{i}_l = -\left[\mathbf{Z}_{TT}^{'}\right]^{-1} \left[C_l^T\right]_t \mathbf{Z}_{TT} \, \mathbf{I}_T \tag{3.8}$$

Step 4. Solve $\mathbf{V}_T$ from

$$\mathbf{i}_l = -\left[\mathbf{Z}_{TT}^{'}\right]^{-1} \left[C_l^T\right]_t \mathbf{Z}_{TT} \, \mathbf{I}_T \tag{3.9}$$

Step 5. Compute the branch current vector $\mathbf{i}_b$ by (3.1).

It is noted that the diakoptic algorithm requires matrix inversions, in practice elimination or triangular factorization techniques can be employed for these inversions.

3.2. Problem Formulation and Approach

Consider a three-phase, balanced radial distribution system consisting of a main feeder, laterals and sublaterals. Fig. 3.2 presents the one-line diagram of such a network (no sublaterals are shown here) where a numbering system for the buses is adopted such that, starting with the substation bus 0, the buses in any open path on the one-line diagram are numbered in increasing order.

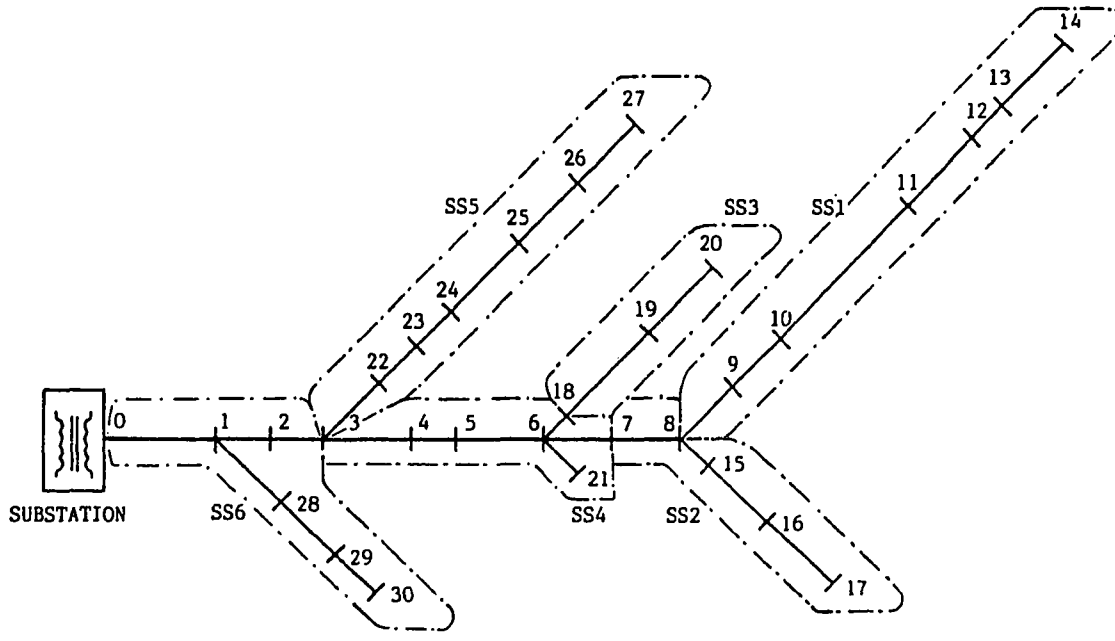

Fig. 3.2. One-line diagram of distribution system

The sizing problem involves the overall savings caused by the reduction in the peak power demand and energy losses while taking the capacitor cost into account, whereas the

tap setting problem concerns only the savings caused by the energy loss reduction for each particular load level; therefore, the tap setting problem can be considered as a subset of the sizing problem. The sizing problem involves the savings in a certain design period T which is divided into nl time intervals T_k, k=1, 2, ...nl, during each of which the load profile is approximated to be constant.

For a given set of conforming load profiles, the overall system is to be optimized such that the net savings

$$S = K_p L_p(S_{ci}^m) + K_e \sum_{k=1}^{nl} L_e^k(S_{ci}^k) - \sum_{i \in C} C_i(S_{ci}^m) \tag{3.10}$$

is maximized with respect to the optimization variables S_{ci}^m and S_{ci}^k, $i \in C$, while satisfying the constraints

$$\mathbf{I}_{BUS}^k = \mathbf{Y}_{BUS}^k \mathbf{V}_{BUS}^k , \quad k=1, 2,...nl, \tag{3.11}$$

$$0 \le S_{ci}^m \le S_{ci}^o, \tag{3.12}$$

$$0 \le S_{ci}^k \le S_{ci}^m \tag{3.13}$$

where

$L_p(S_{ci}^m)$: peak power loss reduction caused by capacitor installation as a function of the maximum capacitor ratings $S_{ci}^m, i \in C$ (corresponding to the maximum load profile),

$L_e^k(S_{ci}^k)$: energy loss reduction during time interval T_k at load level k, caused by applying the optimal tap settings, as a function of the capacitor ratings S_{ci}^k, $i \in C$,

$C_i(S_{ci}^m)$: cost of capacitor installation at bus i as a function of the maximum capacitor rating S_{ci}^m,

K_p, K_e : present worth equivalent conversion factors for system capacity release and energy loss respectively,

$\mathbf{I}_{BUS}^k$: bus current vector injected to the system for load profile k,

$\mathbf{Y}_{BUS}^k$: bus admittance matrix of the system for load profile k,

$\mathbf{V}_{BUS}^k$: bus voltage vector of the system for load profile k ,

S_{ci}^o : maximum capacitor rating permissible as determined by practical considerations, and

C : set of buses where capacitors are installed.

It is noted that the constraints for the peak load level and the off-peak load levels are coupled through (3.13) indicating that the capacitor sizes constitute the upper bounds for the optimal capacitor settings at the off-peak load levels. This weak coupling makes it possible to decompose the problem into the sizing problem and a number of tap setting problems [52].

The tap setting problem can be defined by optimizing

$$S_k(y_{ci}^k) = K_e T_k \sum_i \sum_{j>i} r_{ij}\left(\left|I_{ij}^{ka}\right|^2 - \left|I_{ij}^k\right|^2\right), \quad i \in C, \quad k = 1, 2,\ldots nl, \neq m \quad (3.14)$$

with respect to capacitor admittances y_{ci}^k, $i \in C$, and constrained by (3.11) and (3.13) which can be rewritten as

$$0 \le y_{ci}^k \le y_{ci}^m . \quad (3.15)$$

Herein,

I_{ij}^{k}, I_{ij}^{ko} : line currents from bus i to bus j at load profile k, k =1, 2,...nl, with and without capacitors respectively,

r_{ij} : line resistance between bus i and bus j (r_{ij} = 0 if bus i is not connected to bus j), and

y_{ci}^{m} : maximum capacitor admittance at bus i which corresponds to S_{ci}^{m} in (3.12).

Each of these subproblems can be solved by a "base" algorithm which concerns the optimization for one load level. The solutions correspond to the optimal capacitor settings, y_{ci}^{k*}, for the off-peak levels considered.

The sizing problem is to optimize

$$S_m(y_{ci}^{m}) = K_p \sum_{i} \sum_{j>i} r_{ij}\left(\left|I_{ij}^{mo}\right|^2 - \left|I_{ij}^{m}\right|^2\right) + K_e T_m \sum_{i} \sum_{j>i} r_{ij}\left(\left|I_{ij}^{mo}\right|^2 - \left|I_{ij}^{m}\right|^2\right) -$$

$$\sum_{i \in C} C_i(y_{ci}^{m}) + \sum_{\substack{k=1 \\ k \neq m}}^{nl} S_k(y_{ci}^{m}), \quad i \in C, \quad (3.16)$$

with respect to y_{ci}^{m}, $i \in C$, and constrained by (3.11) and (3.12) which can be written in terms of the corresponding capacitor admittances:

$$0 \leq y_{ci}^{m} \leq y_{ci}^{o} \quad (3.17)$$

Note that in (3.16),

$$S_k(y_{ci}^{m}) = \sup_{y_{ci}^{k} \mid (3.11)} \left\{S_k(y_{ci}^{k}) \mid 0 \leq y_{ci}^{k} \leq y_{ci}^{m}\right\}, \quad i \in C. \quad (3.18)$$

This sizing problem could also be readily solved by the base algorithm if the last summation terms were nonexistent. The presence of these terms requires updating these terms at each iteration as the sizing problem is being solved by the base algorithm. This

updating requires that at each iteration the tap setting problem be solved. However, a simple, heuristic scheme to update S_k and its derivatives will be used as shown in the solution algorithm section. At the end of the optimization process of the sizing problem, the updated y_{ci}^{k} values provide the optimal capacitor settings for each of the load profiles whereas the values of y_{ci}^{m} determine the maximum capacitor ratings.

The optimization procedure for a given load profile is realized by tearing the overall system into subsystems as shown in Fig. 3.2, with each having at most a restricted number of nodes (e.g., seven). Note that the lines of tear go through the nodes so that these nodes occur twice or more often in the subsystems but with their bus load placed in only one subsystem network, e.g., the one located nearest to the substation. The subsystems are interconnected by fictitious impedanceless links. Fig. 3.3 shows a subsystem where the injected currents are composed of the constant power load currents and the link currents which may include the substation current. These link currents function as the interaction variables between the subsystems.

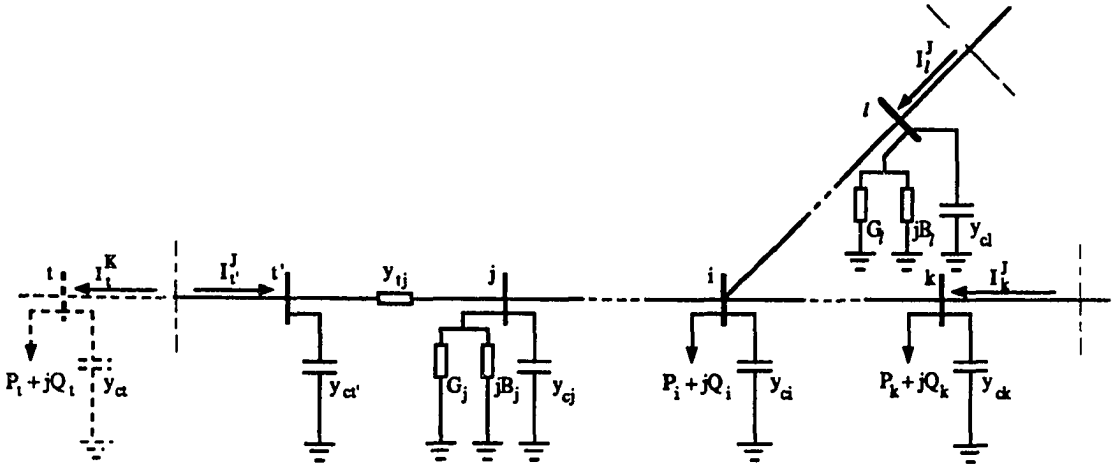

Fig. 3.3. One-line diagram of a subsystem

Distribution loads have been conventionally modeled as conforming active and reactive power sinks. However, experimental results [53] concerning the effect of

capacitor switching on substation variables revealed that switching in of a capacitor bank results in decreased reactive power (as expected) but increased active power injection at the substation. This implies that the overall load of the system tested is voltage sensitive. Therefore, the load sensitivity to voltage has to be known if the economic savings derived from installing capacitor banks constitutes a figure of merit for the capacitor allocation design. Several approaches to model the load are known in the literature, e.g., Ref. 54.

In this study, a part of the distribution loads can be represented by constant impedances and the remainder by constant power sinks whereas the capacitors are invariably modeled as shunt admittances. The resulting equations, however, can be readily modified if some of the loads have to be represented by constant current sinks.

The subsystems are sequentially optimized starting with one of the terminal subsystems located farthest from the substation, and continuing with a subsystem adjacent to one or more optimized subsystems and located on the open path to the substation, through the last subsystem connected directly to the substation. Although the subsystems are individually optimized, precaution is taken in the formulation to reflect the reduction of power and energy loss taking place in the subsystems other than the one being optimized.

The optimization of each subsystem is performed on the basis of the values of the interaction variables at the start of the iteration process. Upon reconnection of all optimized subsystems, the voltages and therefore the link currents acting as the interaction variables are generally different from those obtained in the subsystem optimization process. Thus, the whole system optimization procedure is performed repeatedly until the absolute value of the difference between the overall savings in two consecutive iterations is sufficiently small.

3.3. Subsystem Optimization [55]

A base algorithm to solve the optimization problem for a given *constant* load profile will now be developed for a subsystem. For the constant load profile, the net savings and

constraints for subsystem J in Fig. 3.3 can be written as

$$S_J = (K_p + K_e\tau)\sum_i \sum_{j>i} r_{ij}\left[\left|I_{ij}^o\right|^2 - \left|I_{ij}\right|^2\right] - \sum_{i \in CJ} C_i(y_{ci}) \tag{3.19}$$

and

$$\mathbf{I}_{BJ} = \mathbf{Y}_{BJ}\,\mathbf{V}_{BJ} \tag{3.20}$$

$$0 \le y_{ci} \le y_{ci}^o \tag{3.21}$$

where

$C_i(y_{ci})$: cost function of capacitor at bus i and assumed to be differentiable with respect to y_{ci} ($S_{ci} = V_{rated}^2\, y_{ci}$),

y_{ci} : capacitor admittance at bus i,

$\mathbf{I}_{BJ}$: bus current vector injected to subsystem J and composed of link currents and constant power load currents,

$\mathbf{V}_{BJ}$: bus voltage vector of subsystem J,

$\mathbf{Y}_{BJ}$: bus admittance matrix of subsystem J including constant load impedances and capacitor admittances,

τ : time interval of constant load profile, and

CJ : set of buses in subsystem J where capacitors are installed.

The double summation term in (3.19) not only represents the loss reduction in all branches of subsystem J but also the loss reduction in the branches of those subsystems located between the subsystem considered and the substation. This is because a change in the shunt impedance at any bus theoretically causes all currents in the overall system to change, primarily, however, only in those subsystem branches located on the open path to the substation. Therefore, for purposes of deriving a solution algorithm, the secondary effect of small current changes in all the other branches is neglected.

The maximization of expression (3.19) constrained by (3.20) and (3.21) with y_{ci}, $i \in CJ$, as the optimization variables is a nonlinear programming problem which is here numerically solved by the gradient technique. This method requires an expression for the gradient of the objective function S_J with respect to the capacitor admittances. For this purpose, the branch current is written as

$$I'_{ij} = I_{ij} + \delta I_{ij} \tag{3.22}$$

where δI_{ij} is the current differential in branch ij caused by an incremental change of the capacitor admittances, ∂y_{cl}, and the corresponding voltage differentials δV_l at buses l, $l \geq j$. This current differential can be written as

$$\delta I_{ij} = j \sum_{\substack{l \geq j \\ l \in CJ}} V_l \partial y_{cl} + \sum_{\substack{l \geq j \\ l \in ZJ}} (G_l + jB_l)\delta V_l - \sum_{\substack{l \geq j \\ l \in SJ}} (P_l - jQ_l)\delta V_l^* N_l^{*2} \tag{3.23}$$

with $G_l + jB_l$ and $P_l + jQ_l$ representing respectively the constant load admittance and load power at bus l, and ZJ and SJ constituting respectively the sets of buses in subsystem J to which constant impedance loads and constant power loads are connected.

Expressing the voltages and currents in terms of their real and imaginary components designated by the superscripts 'r' and 'i' respectively, (3.22) is converted into

$$I'_{ij} = (I^r_{ij} + \delta I^r_{ij}) + j(I^i_{ij} + \delta I^i_{ij}). \tag{3.24}$$

Then, considering (3.19) together with (3.22-3.24) and assuming that

$$C_i(y_{ci}) = K_c^o V^2_{rated} u(y_{ci}) + K_c V^2_{rated} y_{ci} \tag{3.25}$$

where K_c^o and K_c are respectively the fixed and marginal capacitor costs, and $u(y_{ci})$ represents the unit step function,

$$\frac{\partial S_J}{\partial y_{ck}} = 2(K_p + K_e\tau)\sum_{i}\sum_{j>i} r_{ij}[(I_{ij}^r + \delta I_{ij}^r)V_k^i - (I_{ij}^i + \delta I_{ij}^i)V_k^r] - K_c V_{rated}^2, \quad k \in CJ . \tag{3.26}$$

Based on the results obtained above, the iterative algorithm is started by incrementing the capacitor admittances (the superscripts between parentheses denote iteration count):

$$y_{ck}^{(n)} = y_{ck}^{(n-1)} + \Delta y_{ck}^{(n)}, \quad k \in CJ , \tag{3.27}$$

with

$$\Delta y_{ck}^{(n)} = \frac{\mu}{N^{(n-1)}}\left[\frac{\partial S_J}{\partial y_{ck}}\right]^{(n-1)} \tag{3.28}$$

where

$$\left[\frac{\partial S_J}{\partial y_{ck}}\right]^{(n-1)} = 2(K_p + K_e\tau)\sum_{i}\sum_{j>i} r_{ij}[I_{ij}^{r\,(n-1)} V_k^{i\,(n-1)} - I_{ij}^{i\,(n-1)} V_k^{r\,(n-1)}] - K_c V_{rated}^2, \tag{3.29}$$

$$N^{(n-1)} = \left\{\sum_{k \in CJ}\left[\left(\frac{\partial S_J}{\partial y_{ck}}\right)^{(n-1)}\right]^2\right\} \tag{3.30}$$

and $\mu(>0)$ is a step size which has to be selected judiciously. Note that at any iteration step, the inequality constraint in (3.21) has to be satisfied. Thus, if at bus k the lower or upper limit of y_{ck} is exceeded, $y_{ck}^{(n)}$ is set to that limit.

Based on (3.22) and (3.23), the currents in branches ij located on the open path

between subsystem J and the substation (including the link current $I_{t'}^{J\,(n)}$, see Fig. 3.3) are incremented as follows:

$$I_{ij}^{(n)} = I_{ij}^{(n-1)} + j \sum_{\substack{l \geq t' \\ l \in CJ}} V_l^{(n-1)} \Delta y_{cl}^{(n)} + \sum_{\substack{l \geq t' \\ l \in ZJ}} (G_l + jB_l)[V_l^{(n-1)} - V_l^{(n-2)}] - \sum_{\substack{l \geq t' \\ l \in SJ}} (P_l - jQ_l)[V_l^{*\,(n-1)} - V_l^{*\,(n-2)}]/[V_l^{*\,(n-1)}]^2 \quad (3.31)$$

Then, Y_{BJ} and I_{BJ} are updated by using respectively $y_{ck}^{(n)}$, $k \in CJ$, and the link current $I_{t'}^{J\,(n)}$ after which the bus voltage vector V_{BJ} is upgraded to satisfy equality constraint (3.20).

The iteration process is continued until the magnitude of the gradient vector

$$N^{(n)} < \varepsilon \quad (3.32)$$

where ε is a preselected small positive number.

3.4. Solution Algorithm

First, the base algorithm to solve the distribution system optimization for a constant load profile is given. Then, an overall algorithm to solve the problem for a varying load profile using the base algorithm as a subroutine is described.

3.4.1. Base Algorithm

Step 1. Compose the bus admittance matrix Y_{BUS} of the overall system including constant load impedances and updated capacitor admittances y_{ck}, $k \in C$.

Step 2. With the substation bus voltage V_0 given, perform a load flow analysis based on (3.11) to find the bus voltage vector V_{BUS} of the overall system (Note that I_{BUS} is composed of the substation current and the injected currents from the constant power loads only).

Step 3. Compute the branch currents

$$I_{ij} = (V_i - V_j)\, y_{ij} \tag{3.33}$$

where y_{ij} is the admittance of the branch connected between buses i and j. Also compute the currents injected to each subsystem network, e.g., at the line of tear between the two subsystems K and J (see Fig. 3.3), the currents I_t^K and $I_{t'}^J$ respectively injected at buses t and t' of subsystems K and J and determined by

$$I_{t'}^J = -I_t^K = (V_t - V_j)\, y_{tj} + y'_{ct} V_t. \tag{3.34}$$

If the iteration count n≥1, and the subsystem just optimized is the last one, compute the overall system savings $S^{(n)}$ and compare if

$$\left| S^{(n)} - S^{(n-1)} \right| < \varepsilon_s \tag{3.35}$$

where ε_s, the savings tolerance used as stopping criterion, is a preselected small positive number. If so, the solution has converged and the iterative computation is terminated.

Step 4. Optimize a subsystem starting with one of the terminal subsystems located farthest from the substation, and continuing with a subsystem adjacent to one or more optimized subsystems and located on the open path to the substation, through the last subsystem connected directly to the substation. The iterative algorithm for the subsystem optimization is given in the previous section. After convergence of each subsystem optimization, return to step 1.

3.4.2. Overall Algorithm

Step 1. Set the initial values of $y_{ci}^m, i \in C$, to those values obtained by optimizing the objective function (3.14) for the peak load level during the entire design period T.

Step 2. Using the base algorithm, maximize S_k in (3.14), k=1, 2,...nl, $\neq$ m, with respect to y_{ci}^{k}, which results in the optimal values $y_{ci}^{k^*}$, $i \in C$.

Step 3a. Use the base algorithm to maximize S_m in (3.16) with respect to y_{ci}^{m}. Due to the existence of S_k and its derivatives, the computation becomes complicated. At each iteration step during the optimization of S_m, if any value of $y_{ci}^{k^*}$ violates the new y_{ci}^{m} value, new values for $y_{ci}^{k^*}$, $i \in C$, should be obtained by solving the tap setting problem for the particular load level k; however, the computation of $y_{ci}^{k^*}$ can be approximated as follows. As the values of y_{ci}^{m}, $i \in C$, change from iteration to iteration, the values of $y_{ci}^{k^*}$ are also modified by applying the following rules (for iteration count n>1):

$$y_{ci}^{k^{*(n)}} = \begin{cases} y_{ci}^{k^{*(n-1)}} & \text{if} \quad y_{ci}^{k^{*(n-1)}} < y_{ci}^{m^{(n)}}, \\ y_{ci}^{m^{(n)}} & \text{if} \quad y_{ci}^{k^{*(n-1)}} \geq y_{ci}^{m^{(n)}}, \end{cases} \qquad i \in C;\ k = 1, 2,...\text{nl}, \neq m. \tag{3.36}$$

Using the modified $y_{ci}^{k^*}$ values, S_k and $S_k^{'}$ can be computed as

$$S_k(y_{ci}^{m^{(n)}}) = S_k(y_{ci}^{k^{*(n)}}), \tag{3.37}$$

$$S_k^{'}(y_{ci}^{m^{(n)}}) = \begin{cases} 0 & \text{if} \quad y_{ci}^{k^{*(n-1)}} < y_{ci}^{m^{(n)}}, \\ S_k^{'}(y_{ci}^{k^{*(n)}}) & \text{if} \quad y_{ci}^{k^{*(n-1)}} \geq y_{ci}^{m^{(n)}}, \end{cases} \qquad i \in C;\ k = 1, 2,...\text{nl}, \neq m. \tag{3.38}$$

Step 3b. At the end of each iteration, verify if

$$|y_{ci}^{m^{(n)}} - y_{ci}^{m^{(n-1)}}| \leq \varepsilon_{ci}, \quad i \in C \tag{3.39}$$

where $\varepsilon_{ci}, i \in C$, the capacitor admittance tolerances used as stopping criterion, are preselected small positive numbers. If so, the solution has converged and the computation is completed; otherwise continue the iterative process until Eqn. (3.39) is satisfied.

3.5. Test Studies

The solution algorithm developed in this paper was implemented on the 30 bus test system used in [1] and shown in Fig. 3.2. The data of the system including loads assumed to correspond with the peak load profile at rated voltage are listed in Table 3.1. Bus load forecasting can be obtained by using any known method, e.g., Ref. 56. Employing the piecewise method, the system was torn into 6 subsystems as indicated by the dashed lines in Fig. 3.2. The following parameters were adopted: K_p = 120 \$/kW, K_e = 0.03 \$/kWh, K_c^o=0, K_c = 5 \$/kVar, T = 1 yr and S_{ci}^o= 1200 kVar, $i \in C$. The load duration curve was assumed to be discretized as listed in Table 3.2. Furthermore, five capacitors are placed at buses 13, 15, 19, 23 and 25.

3.5.1. Constant Power Loads

Using the solution algorithm, the convergence of the optimization process is illustrated by plotting the individual capacitor MVars versus the number of system iterations in Fig. 3.4. The initial capacitor MVars were set to the optimum values obtained from maximizing the energy loss reduction in (3.5) for the maximum load profile without constraint of the capacitor size. It can be seen that for the given load duration curve, some of the final optimal capacitor ratings are significantly smaller than their initial values. These optimal capacitor ratings are listed on the first line (corresponding to 1 pu load level) of Table 3.3.

In Table 3.3, the tap settings provided by the sizing problem solution (indicated by "approx") are compared to and show a consistent agreement with the results (designated by "exact") obtained from solving the tap setting problem for each of the load

profiles where the optimum sizes are used as the upper bound constraint in the optimization process. The difference between the total savings obtained by applying the approximate

Table 3.1. System network & load data [1]

Bus	Bus	Branch Impedance		Load at Bus j & V_{rated}			
i	j	$r_{ij}(\Omega)$	$x_{ij}(\Omega)$	P(kW)	Q(kVar)	G(m℧)	-B(m℧)
0	1	0.5096	1.7030	-	-	-	-
1	2	0.2191	0.0118	522	174	0.9867	0.3289
2	3	0.3485	0.3446	-	-	-	-
3	4	1.1750	1.0214	936	312	1.7694	0.5898
4	5	0.5530	0.4806	-	-	-	-
5	6	1.6625	0.9365	-	-	-	-
6	7	1.3506	0.7608	-	-	-	-
7	8	1.3506	0.7608	-	-	-	-
8	9	1.3259	0.7469	189	63	0.3573	0.1191
9	10	1.3259	0.7469	-	-	-	-
10	11	3.9709	2.2369	336	112	0.6352	0.2117
11	12	1.8549	1.0449	657	219	1.2420	0.4140
12	13	0.7557	0.4257	783	261	1.4802	0.4934
13	14	1.5389	0.8669	729	243	1.3781	0.4594
8	15	0.4752	0.4131	477	159	0.9018	0.3006
15	16	0.7282	0.4102	549	183	1.0378	0.3459
16	17	1.3053	0.7353	477	159	0.9018	0.3006
6	18	0.4838	0.4206	432	144	0.8166	0.2722
18	19	1.5898	1.3818	672	224	1.2703	0.4234
19	20	1.5389	0.8669	495	165	0.9357	0.3119
6	21	0.6048	0.5257	207	69	0.3913	0.1304
3	22	0.5639	0.5575	522	174	0.9868	0.3289
22	23	0.3432	0.3393	1917	639	3.6240	1.2080
23	24	0.5728	0.4979	-	-	-	-
24	25	1.4602	1.2692	1116	372	2.1100	7.0320
25	26	1.0627	0.9237	549	183	1.0380	0.3460
26	27	1.5114	0.8514	792	264	1.4972	0.5000
1	28	0.4659	0.0251	882	294	1.6673	0.5558
28	29	1.6351	0.9211	882	294	1.6673	0.5558
29	30	1.1143	0.6277	882	294	1.6673	0.5558

V_{rated} = 23 kV; Total Load at V_{rated} : P_{total} = 15,003 kW
Q_{total} = 5,001 kVar

Table 3.2. Discretized load duration

Load Level [pu]	Time Period [pu]
1.0	0.2
0.85	0.5
0.7	0.2
0.5	0.1

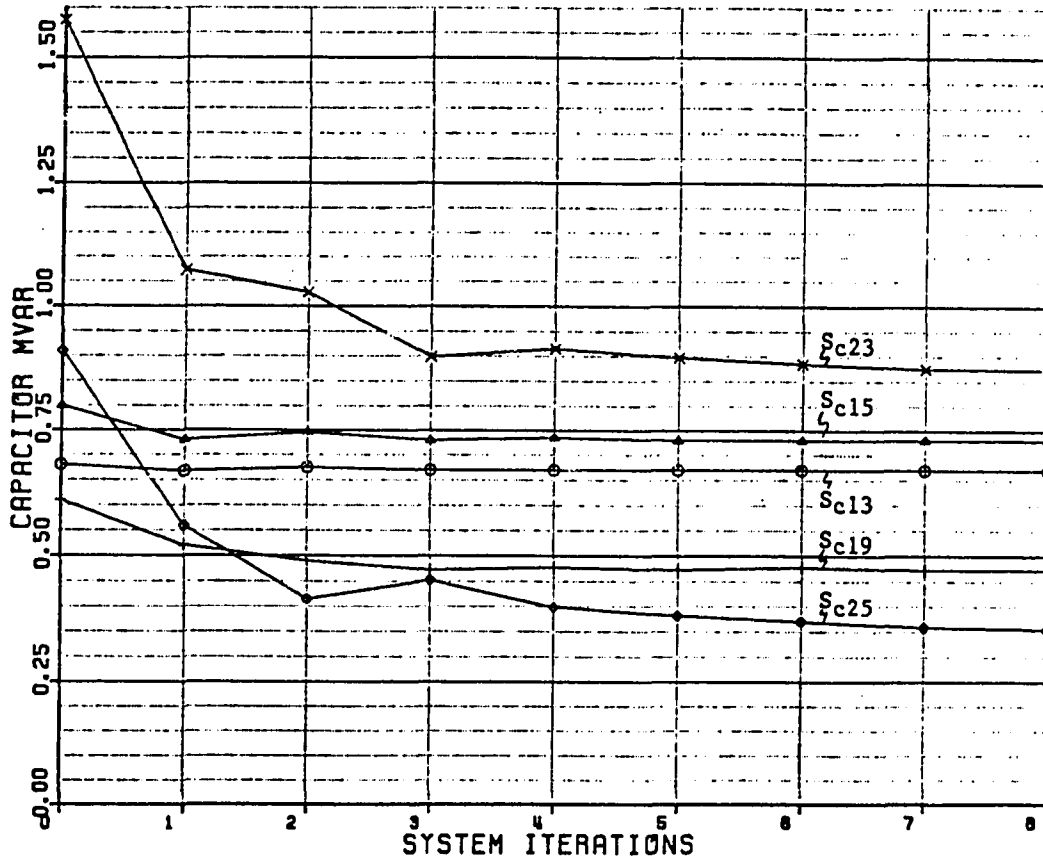

Fig. 3.4. Capacitor MVars vs system iterations for load duration in Table 3.2

Table 3.3. Capacitor tap settings

Load Level [pu]	Capacitor Settings [kVar]									
	C13		C15		C19		C23		C25	
	approx	exact	approx	exact	approx	exact	approx	exact	approx	exact
1.0	670	670	730	730	472	472	874	874	355	355
0.85	670	670	730	730	472	472	874	874	355	355
0.7	520	575	650	594	450	472	874	874	355	354
0.5	380	385	400	371	300	275	820	874	355	334

capacitor settings, S_{approx} = 28.02 k$, and that by using the exact capacitor settings, S_{exact} = 28.07 k$, is negligible. It is noted that a fixed capacitor can be used for any capacitor whose settings do not change during the load profile variation.

3.5.2. Comparison with Constant Impedance Loads

The computation algorithm was also applied to assess the effect of different representations of the distribution loads. Considered were two extreme cases with all individual loads in case (a) represented by constant power sinks, and in case (b) by constant impedances. In both cases, the maximum load level was assumed to prevail for the entire design period. The operating variables before capacitor placement with a substation voltage V_0 = 1.05 pu are summarized in Table 3.4.

Starting from zero capacitor MVars, the results of the iteration process are shown in Figs. 3.5 and 3.6 where the individual capacitor MVars, the total compensating MVar and the savings are plotted versus the number of system iterations. The results after six iterations corresponding with a savings tolerance ε_s of 0.15 k$ and 0.01 k$ respectively for the constant power and impedance loads are listed in Table 3.4.

Comparison of the cases (a) and (b) in Table 3.4 shows that the savings for constant power load is much greater (approximately eight times) than that for constant impedance load. This is because the higher load voltages caused by capacitor installation in both cases result in active currents which are decreasing for constant power load but increasing for constant impedance load whereas the currents or losses without capacitors are larger for constant power load than for constant impedance load.

The advantage of applying diakoptics becomes more apparent when all loads can be represented as constant impedances where the system $\mathbf{Z}_{BUS}$ is required to calculate the bus voltages. By diakoptics the system $\mathbf{Z}_{BUS}$ or $\mathbf{Y}_{BUS}$ can be constructed from the individual subsystem $\mathbf{Z}_{BUS}$ or $\mathbf{Y}_{BUS}$ which will reduce the computation time significantly.

Table 3.4. Comparison of savings

Variable of Interest	a. Const. Power Load		b. Const. Imp. Load	
	Uncomp.	Comp.	Uncomp.	Comp.
S_{c13} (kVar)	--	856	--	683
S_{c15} (kVar)	--	790	--	704
S_{c19} (kVar)	--	409	--	401
S_{c23} (kVar)	--	729	--	462
S_{c25} (kVar)	--	567	--	408
ΣS_{ci}	--	3351	--	2658
Substation:				
P_o (kW)	16213	16044	14917	15249
Q_o (kVar)	6521	3290	5878	3499
Total Loss:				
P_l (kW)	1210	1042	902	853
Q_l (kVar)	1520	1322	1207	1145
Savings(k$)	--	47.87	--	5.9
V_{min} (pu)	0.854	0.891	0.888	0.911

3.6. Conclusions

A piecewise method for obtaining an optimum solution for the size and tap settings of capacitors installed on a radial distribution system has been developed to solve the problem of large system size. The results of the proposed method can be implemented through a centralized substation computer or directly by local controllers [57] performing the capacitor switchings.

The test results show a satisfactory convergence rate of the iterative algorithm. The results also illustrate the significance of proper load representation if the economic savings obtained by capacitor installation is used as a figure of merit for the capacitor design.

The solution algorithm can be used along with a procedure for improving the voltage profile [1] or, it could be modified to include voltage regulators and/or voltage constraints in the formulation for which further research is recommended.

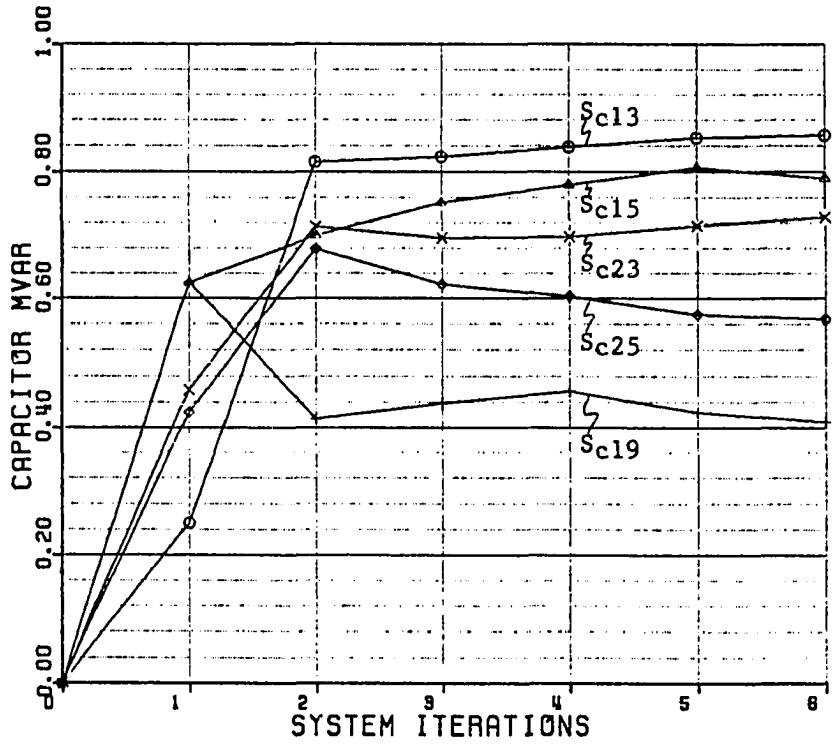

(a)

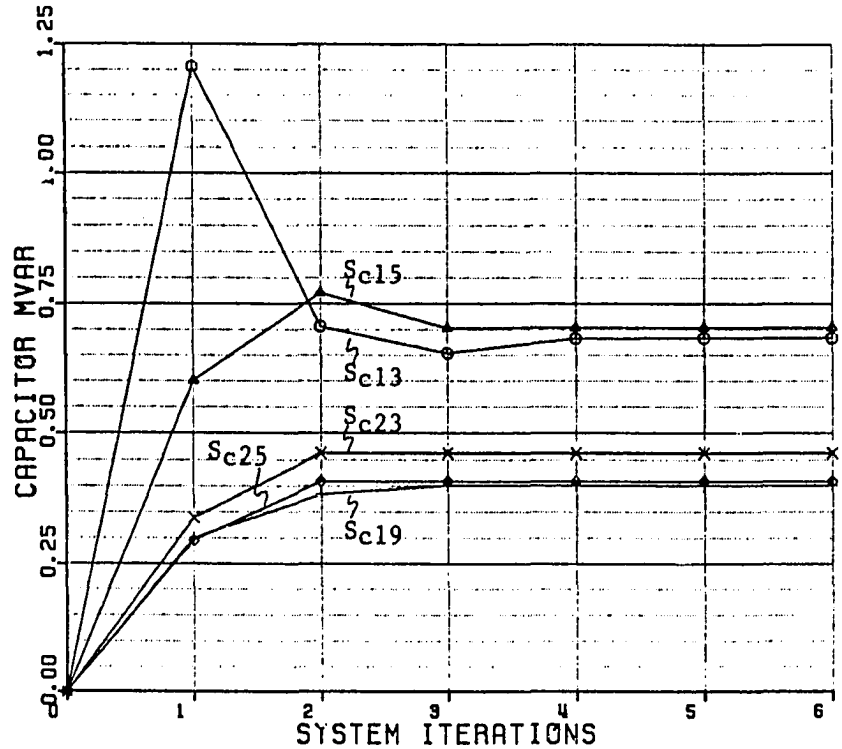

(b)

Fig. 3.5. Capacitor MVars vs system iterations
(a) Constant load power
(b) Constant load impedance

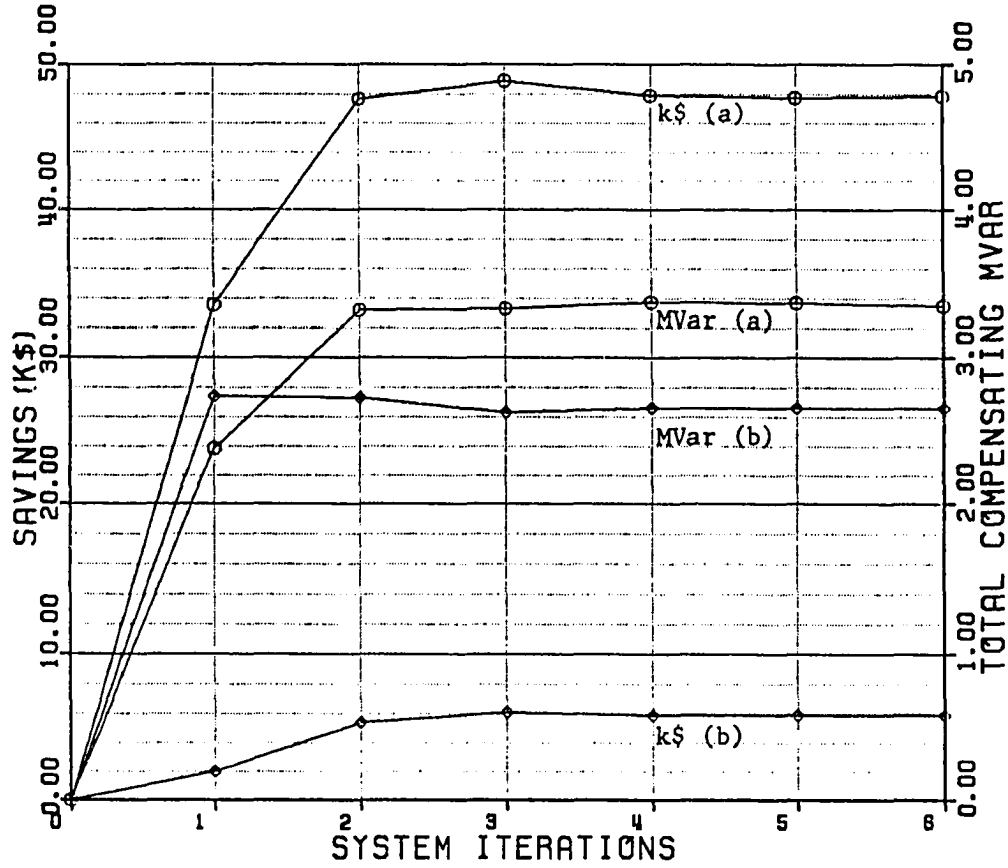

Fig. 3.6. Savings & compensating MVars vs system iterations
(a) Constant load power
(b) Constant load impedance

4. REAL-TIME CONTROL OF DISTRIBUTION CAPACITORS BY NEURAL-NET BASED EXPERT SYSTEM

Artificial intelligence and expert systems will be briefly introduced and emphasis given to an expert system tool called *feed-forward artificial neural network.* The capacitor control problem will be formulated and solved using a neural-net based expert system [58]. An expert system using a two-stage artificial neural network is proposed to control in real time the multitap capacitors installed on a distribution system for a nonconforming load profile such that the system losses are minimized. The required input data are directly obtained from on-line measurements which include the active and reactive line power flows, voltage magnitudes, and the current capacitor settings at certain buses.

A simulation of the expert system has been developed in FORTRAN and validated on a 30 bus distribution system. A practical assumption is taken that the variation of nonconforming load groups ranges discretely from 50% to 100% of their maximum values, and the capacitors have several discrete settings which will be determined in the design process. Comparison between the values estimated by the neural-net based method and the true values computed directly from the optimization method will be made for various cases.

4.1. Tools and Applications of Expert Systems

Expert systems, a kind of artificial intelligence, have attracted widespread interest in recent years. An expert system can be distinguished from other kinds of artificial intelligence in several respects, i.e., it deals with a subject matter of realistic complexity that normally requires a considerable amount of human expertise, it must exhibit high performance in terms of speed and reliability in order to be a useful tool, and it must be capable of justifying solutions and recommendations.

4.1.1. Artificial Intelligence

Artificial intelligence (AI) is concerned with designing an intelligent system that exhibits the characteristics associated with intelligence in human behaviour, e.g., learning, reasoning, solving problems and communicating, which involve such higher mental processes as perceptual learning, memory organization and judgmental reasoning. Research in AI is focused mainly on (a) making systems more useful and (b) understanding intelligence itself; engineering applications are primarily concerned with the first goal.

AI differs markedly from scientific and engineering calculations that are primarily numeric in nature and for which solutions are known that produce satisfactory answers. In contrast, AI's main concern is symbolic processes involving complexity, uncertainty and ambiguity. The processes are usually those for which algorithmic solutions do not exist and a heuristic search is required. AI programs mainly deal with concepts and words, and often do not guarantee an exact solution; some "off" decisions being tolerable as in human problem solving. Moreover, most AI systems employ a separate control structure from the domain knowledge; therefore, it is easier to modify, update and enlarge an AI system than a numerical program. AI components can be visualized by Nilsson's *onion model* [59] which is illustrated in Fig. 4.1. The inner ring depicts the basic elements which are used for the applications shown in the outer ring.

Basic Elements of AI

One of the usual ways of representing problem solving in AI is in terms of a tree configuration. *Heuristic search* may not produce the most optimum path, but can help guide the search which will reduce the search space enormously. Another characteristic of intelligent behaviour is that it does not depend so much on the methods of reasoning, as it is more dependent on the knowledge one has to reason with; this is called *knowledge representation.* The most difficult to model is *common sense and logic.* Common sense is based on a wealth of experience, and logic is important to deduce something (new) from a

set of facts or experiences. The last element of AI includes specific high level languages and software tools developed for different AI application domains; the main programming languages for AI are LISP and PROLOG; however, AI can also be simulated in other high level languages.

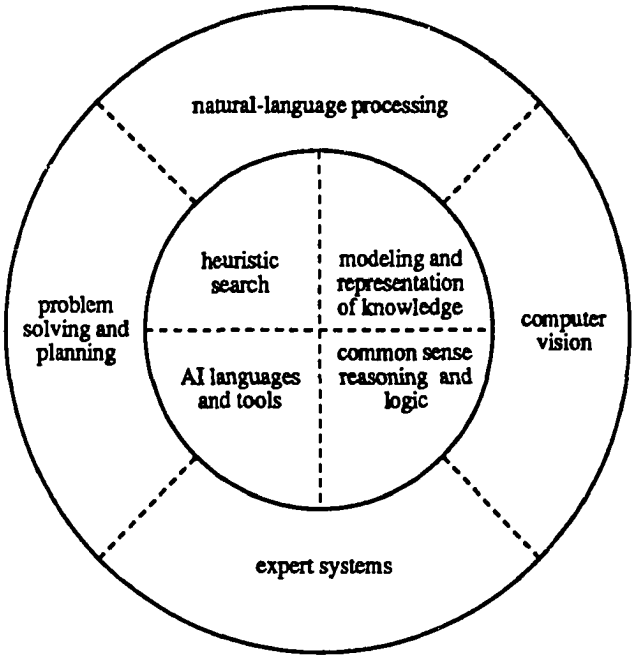

Fig.4.1. Fundamental elements and applications of AI

Principal AI Application Areas

Based on the AI basic elements, four principal AI application areas can be identified. *Natural language processing* is concerned with natural language front ends to computer programs, computer-based speech and text understanding, and related applications. *Computer vision* is concerned with enabling a computer to see, to identify or understand what it sees and to locate what it is looking for. An *expert system* is an artificial intelligence system created to solve a problem in a particular domain; a further description of expert systems is given in the next section. *Problem solving and planning* concerns problems for which there are no experts, but nevertheless computer programs for their

solutions are needed; some of these are more concerned with solution techniques than with knowledge.

4.1.2. Expert Systems

Non-knowledge guided search techniques or computational logic (rule-based search techniques) were successfully used to solve elementary problems or very well structured problems such as games. However, real complex problems are prone to have the characteristic that their search space tends to expand exponentially with the number of parameters involved. For such problems, these older techniques have generally proved to be inadequate and a new approch was needed. This new approach emphasizes knowledge rather than search and has led to the field of knowledge-based systems.

An expert system is basically a computer program that emulates the reasoning process of a human expert or the computing process of a time consuming computer program in a specific domain. It can also handle the uncertainties associated with the use of heuristic rules or real world data. The expert system is a modular program consisting of a *knowledge base*, an *inference engine*, a *user interface*, and sometimes a *global data base* [59]; this basic structure of an expert system is illustrated in Fig. 4.2. The knowledge base contains human expertise describing relations in the domain. The knowledge is generally based on the problem solving expertise developed by a human expert; if it can be stored as production rules, then it is often referred to as the *rule base*. Inference strategies in a rule-based system can be *goal driven* (*backward chaining* method) or *data driven* (*forward chaining method*), or a combination of those. Other knowledge representations include semantic networks, frames, processes and scripts [60]. The inference engine actively uses the data and provides a reasoning strategy and generates solutions for the current problem. The user interface provides communication between the user and the expert system. The data base keeps track of the problem status, the input data for the particular problem, and the relevant problem solving history.

The approaches used in the various expert systems are different implementations of two basic ideas: (1) find ways to efficiently search a space and (2) find ways to transform a large search space into smaller manageable spaces that can be searched efficiently.

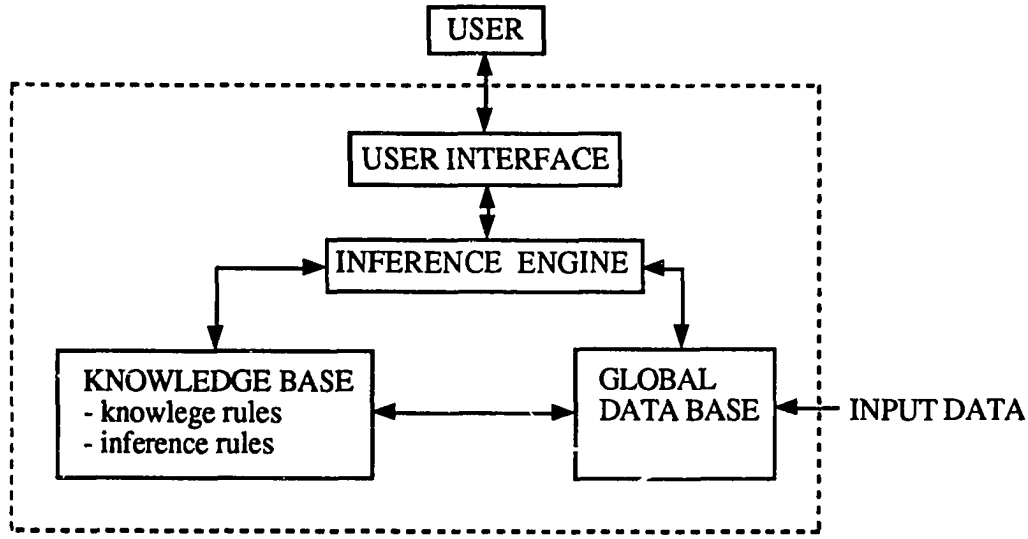

Fig. 4.2. Basic structure of expert system

4.1.3. Artificial Neural Networks

An artificial neural network (ANN), a tool for building an expert system, attempts to achieve good performance via dense interconnection of simple computational elements. An ANN structure is based on our present understanding of biological nervous systems. Neural-net models have greatest potential in areas where many hypotheses are pursued in parallel and high computation rates are required, such as speech and image (pattern) recognition.

An ANN can be defined as a computational model composed of many nonlinear computational elements (*nodes*) operating in parallel and connected by *links* with variable *weights* (a pattern reminiscent of the biological neural network). A node sums several weighted inputs and passes the result through a nonlinearity, e.g. hard-limiter (step function), threshold logic and sigmoid. The node is characterized by an internal threshold

and the type of the nonlinearity. In general, ANN models are specified by the node characteristics, node connections and training or learning rules; these rules specify an initial set of weights and thresholds and indicate how weights and thresholds should be adapted during training to improve the overall network performance.

Recently, the primary application of ANN is in the pattern recognition area. Considered as a method for pattern recognition, ANN has several advantages over the other existing methods, i. e., it has a high computation speed provided by massive parallelism, it has a greater degree of robustness/fault tolerance than Von Neumann sequential computers, it adapts easily and can be continuously trained, and it is good not only for classifying old regions, but also for predicting new regions. Some models are capable of synthesizing a complex, transparent, and highly nonlinear mapping from input to output.

Several methodologies of the artificial neural network have been developed starting from the perceptron idea of Rosenblatt [61] which later is classified into single and multilayer perceptrons. Recent studies include models and methodologies developed by Hopfield, Carpenter-Grossberg, Rumelhart, Kohonen and Kak [61]. One of these is based on a feed-forward layered machine of the perceptron type as developed by Rumelhart et al. [62]. This model is capable of synthesizing a complex and nonlinear mapping from input to output which is the case for the proposed capacitor control. It was shown that the AN network can indeed train itself autonomously as desired by using nonlinear functions for the activation of the "neurons" and by applying a backward error propagation algorithm to update the internal representation variables of the neural network (weight and threshold parameters) until a proper recognition capability has been obtained.

Feed-forward Artificial Neural Network

An AN network consists basically of three layers: input layer, output layer and one or more hidden layers. The idea underlying the design of the network is that known input data are supplied to the input layer units, then by minimizing the difference between the

known output and the computed output with respect to the internal representation parameters, the input-output pattern can be recorded into the internal representation units. Provided that there are enough hidden units, learning patterns can always be encoded in a form such that the appropriate output pattern can be generated from any given input pattern.

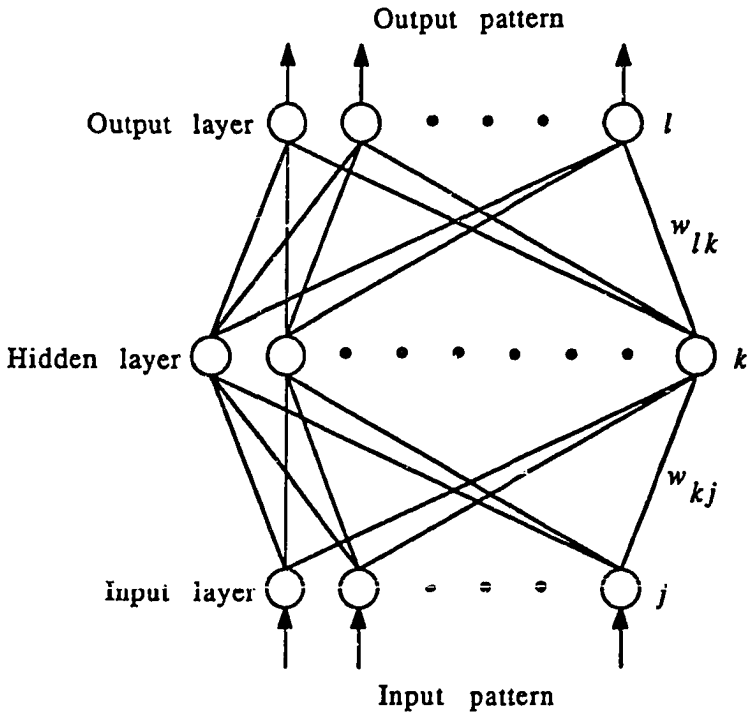

Fig. 4.3. A three layer feed-forward artificial neural network

A typical three layer feed-forward network is shown in Fig. 4.3. In the following, the subscripts j, k and l refer to any unit in the input layer, hidden layer and output layer respectively. The total input to unit k in the hidden layer or to unit l in the output layer is

$$i_r = \sum_s w_{rs} o_s \ , \qquad r = k, l \ ; \ s = j, k \tag{4.1}$$

where o_s represents the output of unit s, s=j, k, in the input/hidden layer and w_{rs} is the weight for o_s going to unit r, r=k, l, in the hidden/output layer. The output of a particular

unit r is

$$o_r = f(i_r), \qquad r = k, l \tag{4.2}$$

where f is the activation function of unit r. An activation function most commonly used in dealing with nonlinear mapping is the sigmoidal function whose input-output relationship is expressed by

$$o_r = \frac{A}{1 + e^{-(i_r - t_r)/\theta_r}}, \qquad r = k, l \tag{4.3}$$

where

A : the maximum output of the activation function whose value is determined by the possible maximum value of the output variable,

t_r : the threshold value of unit r, $r=k, l$, whose function is to position the transition region of the f function, and

θ_r : a variable which determines the abruptness of the transition of function f from 0 to A.

In the learning process, the network is exposed to a set of p patterns, each pattern consists of an input pattern and the corresponding desired output pattern. The pattern number will be represented in the formulation by an additional subscript p. The weights and thresholds are then adjusted to a set of values which can best represent the input-output relationship of the given learning pattern p by minimizing the total error function E_p,

$$E_p = \frac{1}{2} \sum_l (o_l^o - o_l)^2 \tag{4.4}$$

where o_l^o is the known output for unit l in the output layer and o_l is the computed output.

The iterative determination of the weights is usually initiated by setting the weights to some small random values [61]. The weight adjustments are then made by applying the

generalized delta rule which is based on the well-known gradient minimization method [62]. Weights between unit k in the hidden layer and unit l in the output layer (or between unit j in the input layer and unit k in the hidden layer) can be updated by

$$w_{rs}^{(n+1)} = w_{rs}^{(n)} + \eta\, \delta_r\, o_s^{(n)}, \qquad r = k, l;\ s = j, k \tag{4.5}$$

where n is the iteration number, η is the learning rate constant, and δ_r is an error signal of output unit r. The error signal δ_l for updating weights between the hidden layer and the output layer can be obtained by multiplying the difference between the real output and the computed output by the derivative of o_l with respect to i_l [62]:

$$\delta_l = (o_l^0 - o_l)\, o_l (1 - \frac{o_l}{A}) \tag{4.6}$$

Because no known ouput is specified for the hidden units, the error signal δ_k of a hidden unit k for updating weights between the input layer and the hidden layer is determined recursively in terms of the error signals of the output units to which the hidden unit k is directly connected, and the weights of those connections [62]:

$$\delta_k = o_k (1 - \frac{o_k}{A}) \sum_l \delta_l w_{lk} \tag{4.7}$$

The convergence rate can be improved by adding a momentum term [62] to Eqn. (4.5):

$$w_{rs}^{(n+1)} = w_{rs}^{(n)} + \eta \delta_r\, o_s^{(n)} + \alpha (w_{rs}^{(n)} - w_{rs}^{(n-1)}), \quad r = k, l;\ s = j, k \tag{4.8}$$

where α is the momentum factor which reflects the effect of the previous weights on the current weight change. The computation time needed to obtain the weights in a particular AN network depends mainly on the number of input, hidden and output units, the number of training patterns, the extent of nonlinearity of the input-output relationship, and the required accuracy.

The thresholds are learned by equating θ_r , $r=k,l,$ to a weight w_{rt} connecting the unit r to an imaginary lower layer unit t which is always turned on to give unity output [62]. The weight w_{rt} is iteratively updated in the same manner as the other weights by using Eqn. (4.8) along with Eqn. (4.6) or (4.7).

The iterative algorithm for obtaining the set of weight and threshold values which best represents the input-output relationship is performed by applying Eqns. (4.1)-(4.8) to all training patterns sequentially and repeating the process until

$$E^{(n)} - E^{(n-1)} \leq \Delta E \tag{4.9}$$

where

$$E = \sum_p E_p$$

and the error tolerance ΔE , a preselected very small positive number, is used as a stopping criterion. The algorithm does not always guarantee a global minimum solution. Convergence to a local minimum can be identified by a large total error value E, and can be corrected by selecting different initial values for the thresholds and weights. The number of hidden units, η and α are to be determined by experience; however, η and α values generally vary between 0 and 1.

4.2. Capacitor Control Problem Formulation

The location and maximum ratings of capacitors installed on a distribution system are considered to be known from the capacitor design process where the peak power demand and varying load profile as well as the capacitor cost have been taken into account. These maximum ratings will constitute the upper bound for the capacitor kVars in controlling the multitap capacitors when load variations occur.

The measured variables include the active line power P, reactive line power Q, and voltage magnitude $|V|$ at certain buses of the distribution system as well as the current

capacitor settings. For a given set of these measurement data, the new capacitor settings have to be determined such that the savings

$$S = K_e L_e(S_{ci}) \tag{4.10}$$

is maximized with respect to the optimization variable S_{ci}, $i \in C$, while satisfying the constraints

$$I_{BUS} = Y_{BUS} V_{BUS}, \tag{4.11}$$

$$0 \le S_{ci} \le S_{max} \tag{4.12}$$

where

$L_e(S_{ci})$: the energy loss reduction as a function of the capacitor kVars S_{ci}, $i \in C$, caused by the capacitor installation during a time period of constant load profile,

K_e : the present worth equivalent conversion factor for energy loss, and

C : the set of buses where the capacitors are installed.

Thus, a computationally efficient control procedure for selecting the optimal capacitor tap positions for a given load profile is to be developed where the input variables are composed of a limited number of practical measurements without providing direct information on the individual loads themselves.

4.3. Capacitor Control Network

It is generally known that the convergence rate of the learning process of an AN network heavily depends on the extent of nonlinearity of the input-output relationship. The error in the prediction of the AN network output also becomes relatively large if this relationship is highly nonlinear. In such cases, it is recommended to decompose the AN network into several stages such that the nonlinearity of the input-output relationship for each stage is substantially reduced.

4.3.1. Network Configuration

Considering the highly nonlinear input-output relationship in the capacitor control problem, it is desirable to utilize a cascade connection of two AN networks as shown in Fig. 4.4. In the first stage, the load profile has to be predicted from the measured active and

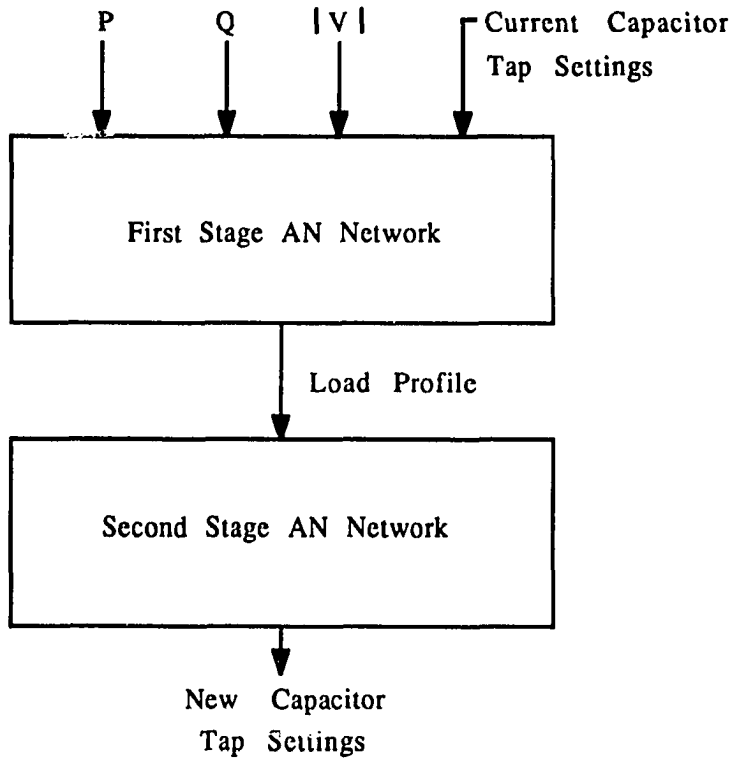

Fig. 4.4. Block diagram of control network

reactive line powers, voltage magnitudes and the current capacitor settings. In the second stage, the optimal capacitor tap settings have to be selected from the load profile predicted by the first stage. Basically, both stages of the AN network have continuous input and output values; however, both outputs are discretized into several levels to enchance the accuracy of the results.

First Stage AN Network

The distribution system is divided into several subsystems whose aggregated loads

do not necessarily vary in the same proportion over the load cycle. The subsystem loads are expressed in percents of their peak values. If the occurence of all nonoptimal combinations of load levels and capacitor settings throughout the entire distribution system is to be considered, the number of those combinations will be excessively large which will complicate the training process. This would also introduce a high probability that the input-output relationship is not unique, i.e., several input patterns may generate the same output pattern and vice versa.

Consequently, the problem is decomposed into several sub-problems, each of which concerns the determination of the load level in a corresponding subsystem only. This load level is estimated from the measured active and reactive line powers P and Q, the voltage magnitudes $|V|$ at certain terminals, and the current settings of the capacitors installed on the system. Thus it is implied that the energy loss in the distribution lines is small compared to the load energy. Note that using Q ,$|V|$ and the capacitor settings besides P as input provides the capability to include cases where the reactive load power varies independently from the active load power. Although the role of $|V|$ in determining the load levels is of little significance, it is essential for a voltage regulator control which is considered beyond the scope of this study.

Fig. 4.5 shows a number of separate parallel AN networks, each of which corresponds to a subsystem. Each AN network is provided with a prelayer (not shown in Fig. 4.3) of which the number of nodes equals the number of measurement variables and capacitors installed on the system. All continuous valued measurements and capacitor settings are supplied to the prelayer which selects the input variables appropriate to the particular AN network. A measured line power going into (out of) the corresponding subsystem is given unity (minus unity) weight between the prelayer and input layer, whereas zero weight is assigned to prevent inappropriate variables from being fed to the AN network.

The output of each AN network representing the subsytem load level is generated

by *nl* output units where *nl* is the number of feasible load levels in the particular subsystem. Thus the output is expressed in *nl* digits, each of which represents a load level and only one of those digits should have a value of "1" indicating a load at a particular level. In some cases two of the *nl* digits may assume the value "1" implying that based on the available knowledge, two solutions are possible for the particular input. If this occurs,

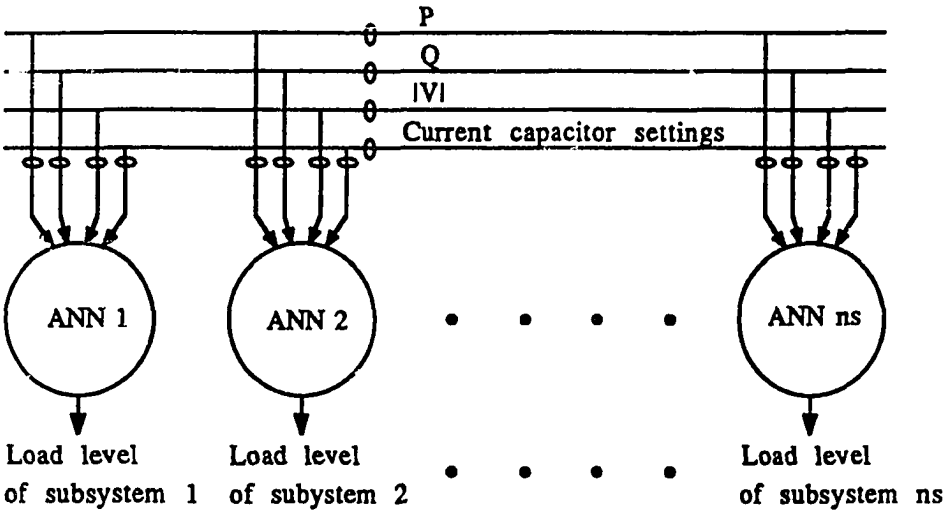

Fig. 4.5. First stage AN network

the higher load level will be selected because overcompensation will have the advantage of a higher power factor than undercompensation.

The number of hidden units can be approximated by $ni(2ni+1)$ where *ni* is the number of input units [61]. In practice, the exact value will be determined by experience. For this stage, the training data are generated by computing the measurement variables for several optimal and nonoptimal combinations of load levels and capacitor settings.

Second Stage AN Network

In this stage, an individual AN network is provided for each capacitor installed on the distribution system as shown in Fig. 4.6. Each AN network accepts the load levels of all subsystems as input and provides the control measures for the corresponding capacitor.

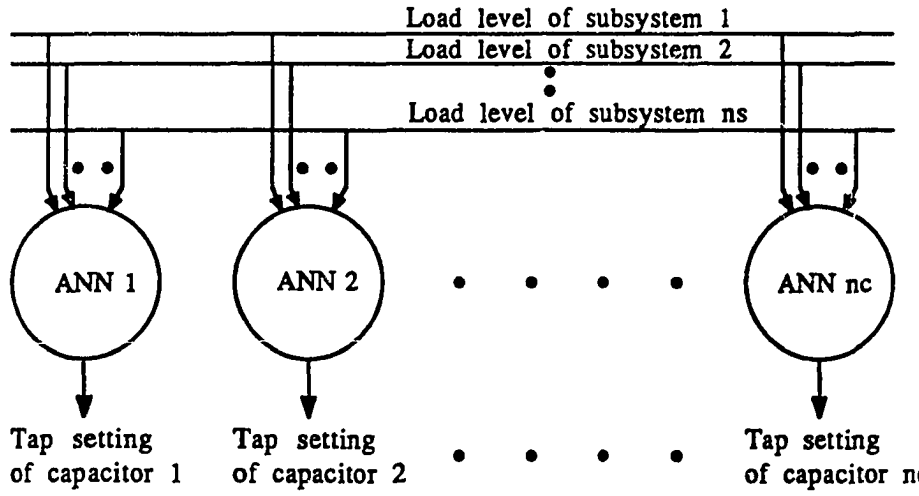

Fig. 4.6. Second stage AN network

The number of input units per AN network corresponds with the number of subsystems with nonconforming aggregated loads. The output of each AN network generated by *nt* output units represents the capacitor tap position and is expressed by *nt* digits where *nt* is the number of the capacitor settings. Each digit represents a capacitor tap setting: a "1" or "0" indicates whether or not the corresponding capacitor switch is closed. For this stage, the training data are generated by conducting an optimization process for all combinations of feasible levels of the load groups.

4.3.2. Training Procedure

1. Obtain a set of training data for the first stage AN network by computing the measurement variables for a preselected set of load profiles and capacitor settings.

2. Obtain a set of training data for the second stage AN network by performing the capacitor control optimization procedure for a preselected set of load profiles.

3. Train separately both stages 1 and 2 of the control network until a satisfactory convergence is observed, then record all the weight and threshold values. Watch for cases where the iteration converges to a local minimum, these conditions can be remedied by

repeating the training procedure with different initial values for the weights and thresholds. Adjusting the iteration parameters η and α may also improve the algorithm to converge faster to the correct solution.

4. Using the weight and threshold values obtained in step 3, the load profile and the corresponding optimal capacitor settings can be determined for any given set of measurements.

4.4. Test Studies

The solution algorithm developed in this study was implemented on the same 30 bus test system used in the capacitor design algorithm described in Chapter 3 (Fig. 3.1). Optimum capacitor settings have been obtained in Chapter 3; their optimum locations can be obtained by applying the conventional exhaustive combinatorial method [1] or the gradient search method proposed by Wu and Baran [15,16].

4.4.1. Distribution System Modeling

The torn system with the installed measurement devices (M) and the optimum capacitors (C) is shown in Fig. 4.7. The data of the system including loads are listed in Table 3.1. The system is torn into 6 subsystems (SS1-SS6) as indicated in the figure where each subsystem has an aggregated load which is nonconforming to the remaining system load. The location of the measuring devices (M1-M6) and 5 capacitors (C1-C5) is also shown.

The aggregated loads of the subsystems were assumed to change discretely among four levels with the active and reactive load powers in each of the subsystems varying proportionally. All loads were represented by constant power sinks in the power system simulation.

The maximum capacitor ratings are set at the assumed commercially available capacitor kVars nearest the optimum kVar values obtained from the design process

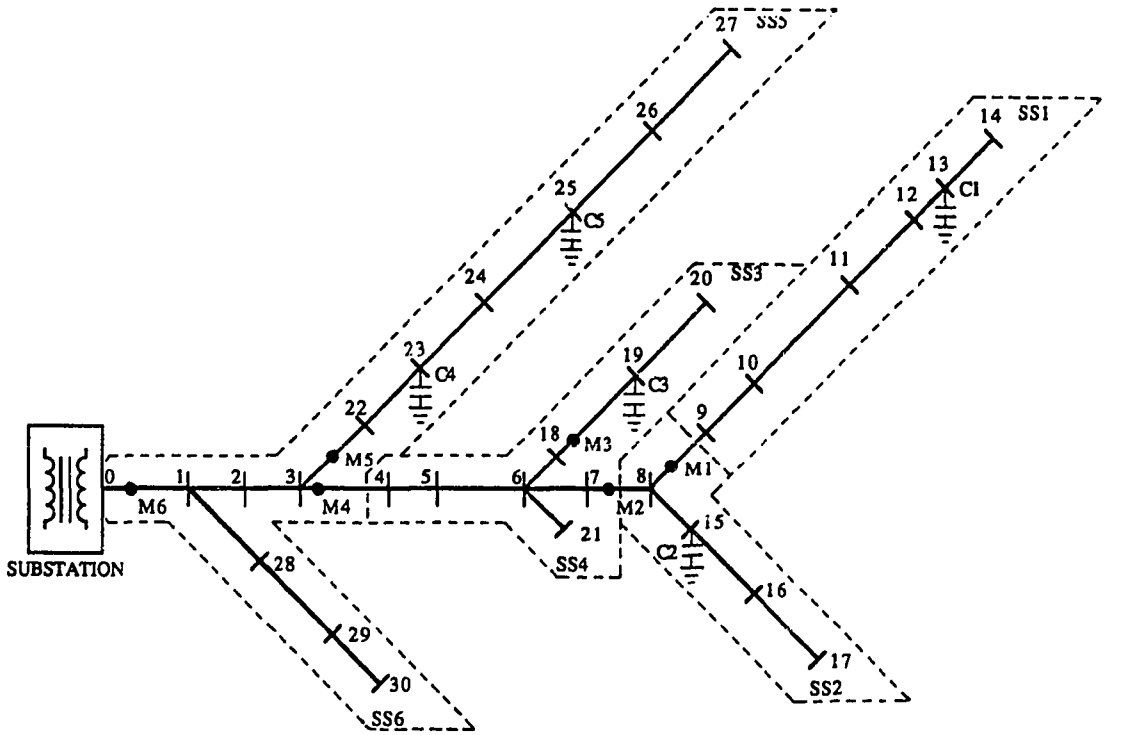

Fig. 4.7. Distribution test system with the measuring device and capacitor locations.

[48]. The minimum capacitor settings are fixed at some commercially available kVar values nearest the lowest capacitor ratings obtained from the optimization process for the minimum load profile. Between these maximum and minimum settings, another two capacitor settings are assigned such that the differences of the capacitor kVars between one setting to another are equal (see Table 4.1).

4.4.2. Simulation Results

In this application, the outputs of the AN networks representing load levels in the 1st stage and capacitor settings in the 2nd stage are determined by combinations of "0" and "1" values, each of which generated by the output units. Therefore, the value of A representing the maximum output of an activation function is less significant and was set equal to unity. The first stage AN network in Fig. 4.5 has 6 separate AN networks, each of which corresponds to a subsystem with a nonconforming aggregated load. Considering

Table 4.1. Capacitor kVars at different tap positions

Tap Position	Capacitor kVar				
	Cap. #1 at bus 14	Cap. #2 at bus 15	Cap. #3 at bus 19	Cap #4 at bus 23	Cap #5 at bus 25
1	875	875	500	fixed at 750	600
2	700	700	425		525
3	525	525	350		450
4	350	350	275		375

that each load group has four feasible levels, the output of each AN network is discretized into four levels where each level is represented by one digit. Thus, each AN network has 4 output units. The number of hidden units, 24 per AN network, was determined by trial and error. It has to be large enough to form a decision region that is as complex as required for the given problem. However, it should not be too large that the many weights required cannot be reliably estimated from the available training data.

For each AN network, 28 (the number of hidden and output units) threshold parameters have to be generated. The number of weights is found from the product of the number of hidden units and the sum of input and output units.

The training data for the first stage AN network were generated by calculating P, Q and $|V|$ at the measurement points for all feasible combinations of load levels and capacitor settings in each of the subsystems. As expected, the effect of adjusting a capacitor setting on the values of P and $|V|$ while maintaining the load profile is much less significant than that on Q. The training process showed a satisfactory convergence rate for all training patterns. The most effective values for η and α were found to be 0.7 and 0.5 respectively.

The second stage AN network in Fig. 4.6 now has 5 separate AN networks, each of which estimates the tap setting of the corresponding capacitor. Each AN network has an output of 4 digits whose values are either 1 or 0; the "1" and "0" values refer to a

connected and disconnected tap position respectively. Each of the 5 AN networks has 6 input nodes corresponding to the number of subsystems, 4 output units, and 32 hidden units. This leads to 320 weights and 36 thresholds whose values have to be determined iteratively.

For the second stage, a set of training patterns was generated by applying the operational optimization process for each load profile. In this example, the set consists of 64 patterns which are found as follows. The aggregated loads in subsystems 1, 2, 3, and 4 were assumed to occur independently at either 50% or 100% of their peak values whereas the percent loads in subsystems 5 and 6 were considered to vary proportionally and take on any value of 50%, 70%, 85% or 100%. The training load patterns are obtained by forming all possible combinations of the subsystem load levels. The training process for this stage also showed a satisfactory convergence rate with $\eta = 0.6$ and $\alpha = 0.5$. In these test studies, the initial weights and thresholds were set to some random values near zero. The final weight and threshold values for any of the AN networks were obtained in less than 200 CPU seconds (on IBM 3070/MVS). The ranges of the weight and threshold values for each of the AN networks are listed in Table 4.2.

The performance of the control network is illustrated for 20 different cases. The first 5 cases refer to input patterns previously used in the training session whereas the patterns in cases 6-20 have not been encountered before. Fig. 4.8 shows the discretized subsystem loads in percents which were estimated by feeding the continuous measurement variables into the first stage AN network. The true continuous subsystem loads in percents were obtained by simulation of the distribution system. Feeding the discretized subsystem loads estimated by the first stage into the second stage AN network resulted in the discretized capacitor settings in kVars as shown in Fig. 4.9. The true discretized capacitor settings were found by rounding the continuous capacitor values obtained from an optimization process off to the nearest available settings. It can be

Table 4.2. Minimum and maximum weight and threshold values

Stage - ANN #	Weight		Threshold	
	min.	max.	min.	max.
1-1	-18.86	+20.00	-3.73	+7.35
1-2	-51.43	+50.64	-8.00	+9.99
1-3	-44.20	+44.70	-4.88	+10.70
1-4	-43.47	+46.36	-8.62	+10.97
1-5	-13.15	+15.66	-6.81	+5.39
1-6	-26.64	+28.63	-8.85	+9.96
2-1	-3.33	+3.45	-0.93	+1.36
2-2	-18.66	+13.56	-15.77	+26.84
2-3	-19.98	+15.27	-19.98	+11.53
2-4	-6.88	+7.55	-13.83	+8.16

observed that in all cases the load profile and the capacitor settings estimated by the expert system are identical or very close (no more than one step for the capacitor settings) to the true values. The computation of any of the optimal capacitor settings was performed in an average of 2.8 CPU seconds.

The estimated discretized capacitor settings in kVars are again listed in Table 4.3, but now compared with the true continuous optimum values. The table also shows the corresponding energy savings in k$/year obtained by the expert system control and that computed by the optimization method using the true continuous capacitor kVars. This comparison shows the relatively small difference in the savings which suggests the adequacy of the proposed capacitor control method.

4.5. Conclusions

A new approach using an artificial neural network has been developed for the real-time control of capacitors installed on distribution systems. From the measurements at certain buses, the control network provides the capacitor settings such that the system losses are minimized for a nonconformably varying load profile.

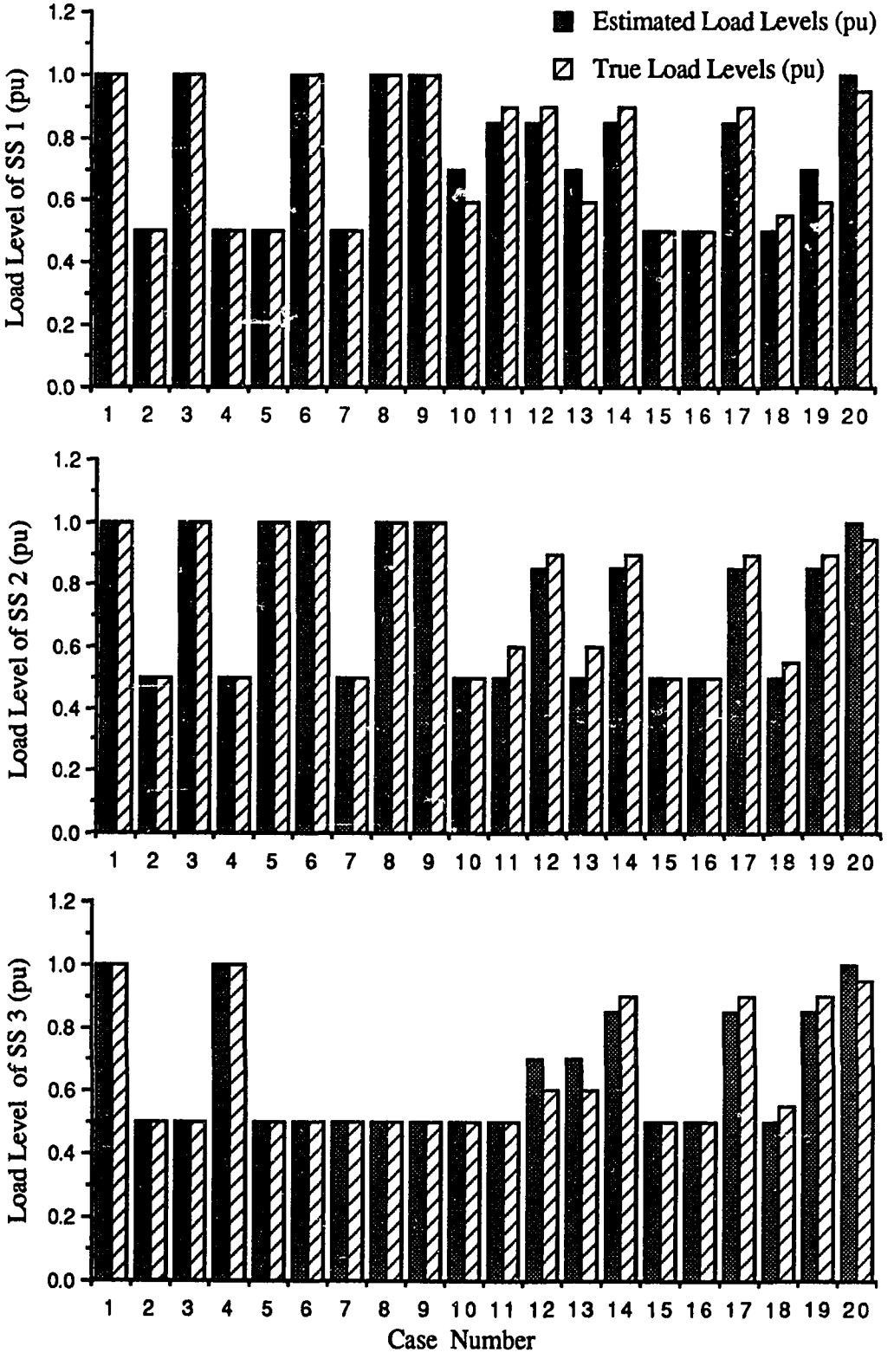

continued ...

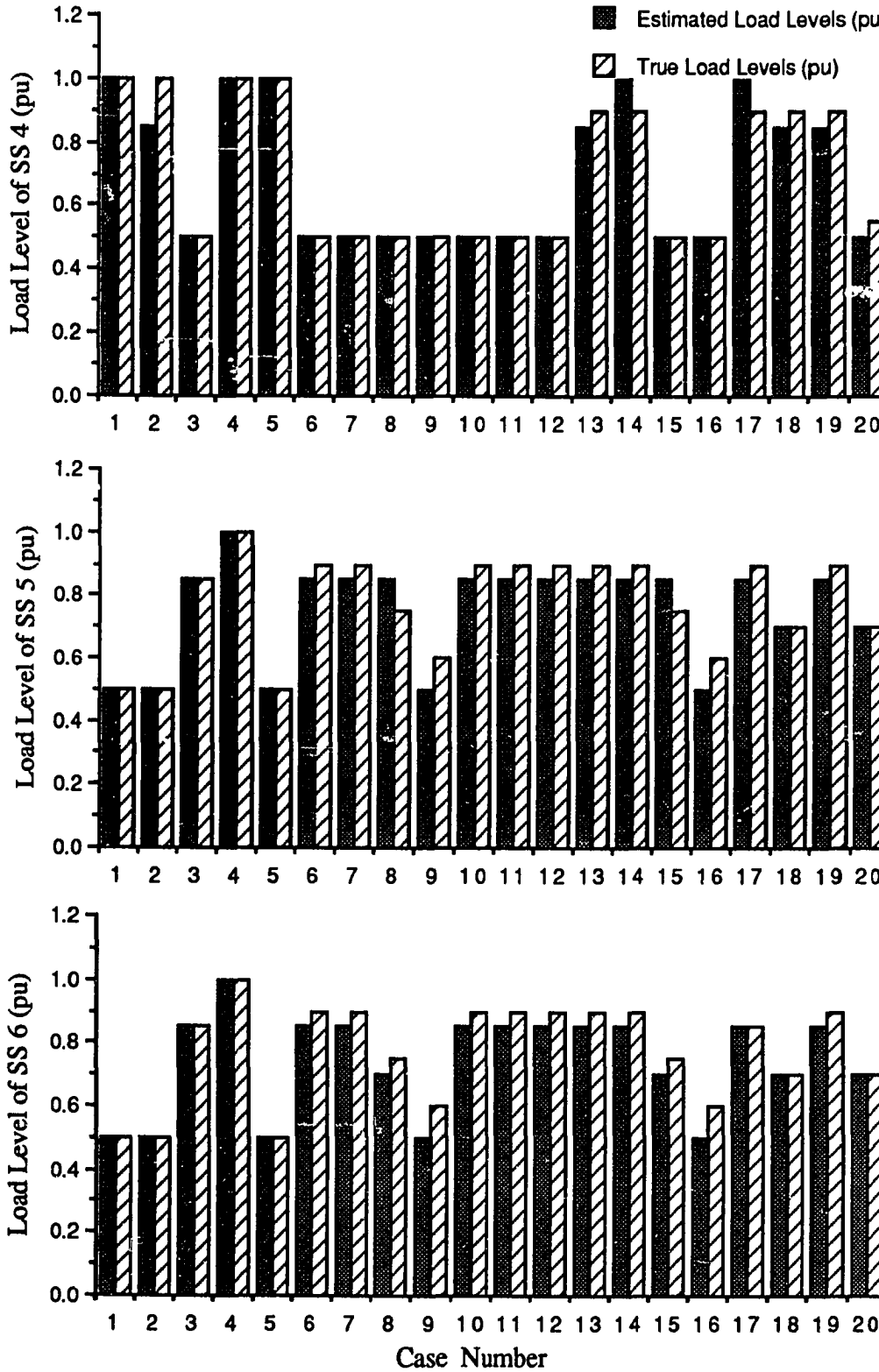

Fig. 4.8. Comparison between estimated and true load levels of the subsystems

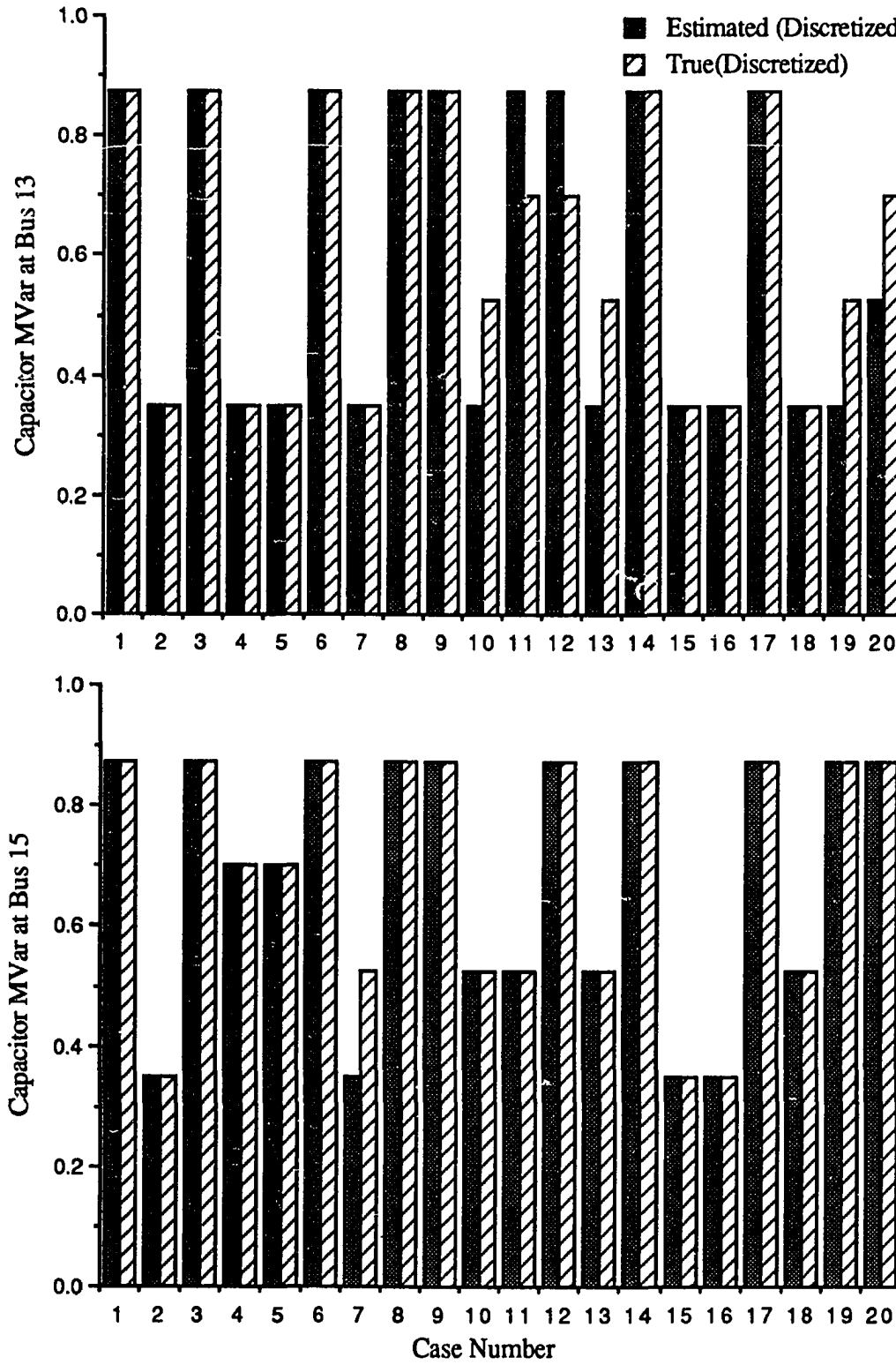

continued ...

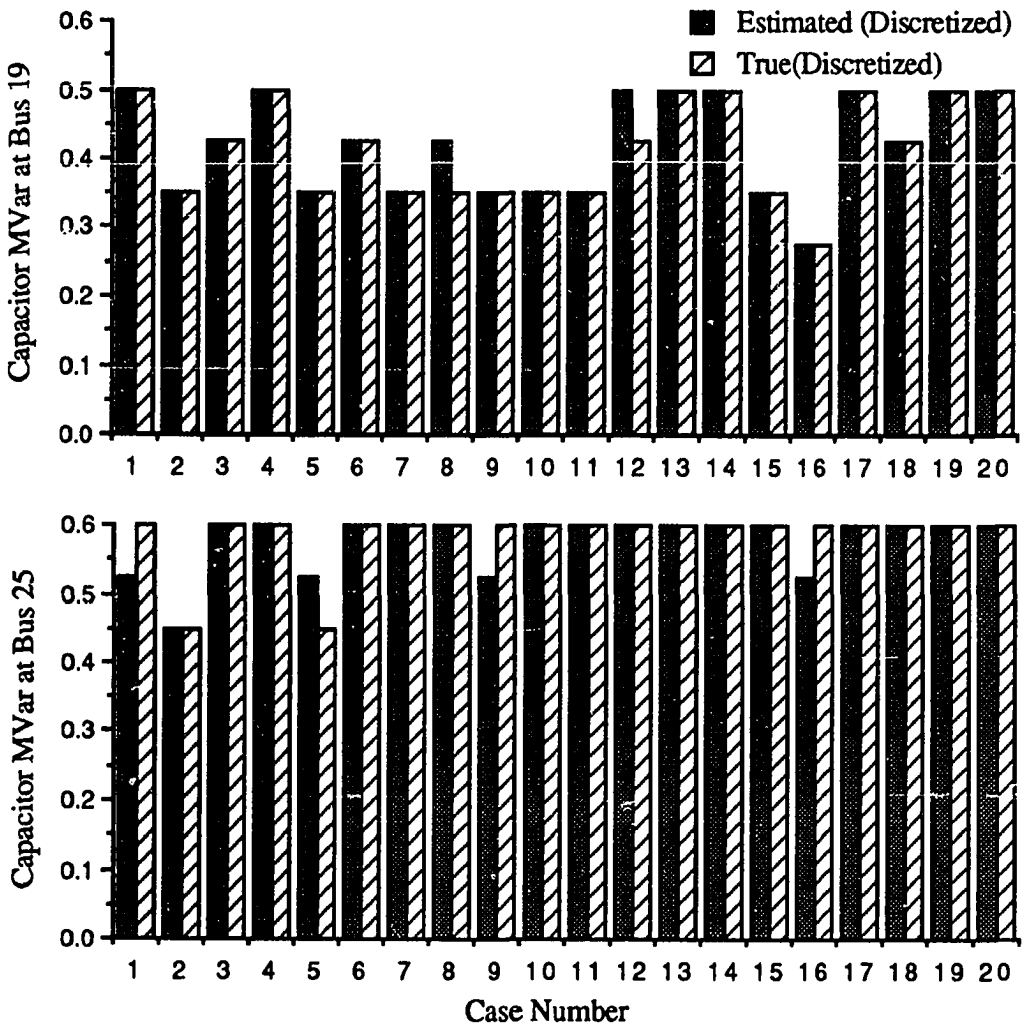

Fig. 4.9. Comparison between estimated and true settings of the capacitors.

Featuring two stages of the neural network, this approach can synthesize a highly nonlinear optimization process. In the first stage, the load profile is determined from a limited number of measurement data as well as the current capacitor settings. In the second stage, the optimal capacitor settings are found from the load profile identified in the first stage.

The control network has been tested on a 30 bus distribution system with quite satisfactory results. This method requires much less computation time if compared with that for an optimization process; it does not involve any iteration procedure. Therefore, it is

Table 4.3. Optimal capacitor settings & savings

Case#	Optimal Capacitor Settings (kVar)										Savings (k$/yr)	
	Estimated (Discretized)					True (Continuous)						
	C1	C2	C3	C4	C5	C1	C2	C3	C4	C5	Estimated	True
1	875	875	500	750	525	875	875	500	750	600	37.7	38.8
2	350	350	350	750	450	377	428	357	750	450	10.1	10.7
3	875	875	425	750	600	850	861	423	750	600	35.5	36.7
4	350	700	500	750	600	410	617	500	750	600	19.7	20.7
5	350	700	350	750	525	381	740	377	750	457	14.5	15.1
6	875	875	425	750	600	869	861	442	750	600	36.3	37.7
7	350	350	350	750	600	414	440	356	750	600	13.0	13.7
8	875	875	425	750	600	840	875	374	750	600	33.7	34.6
9	875	875	350	750	450	831	830	342	750	592	30.8	31.7
10	350	525	350	750	600	488	481	358	750	600	15.0	16.0
11	875	525	350	750	600	746	605	380	750	600	25.9	26.7
12	875	875	500	750	600	769	804	430	750	600	31.6	32.0
13	350	525	500	750	600	494	514	500	750	600	18.2	19.4
14	875	875	500	750	600	788	875	500	750	600	37.2	37.6
15	350	350	350	750	600	393	404	336	750	600	11.1	11.7
16	350	350	275	750	525	392	388	284	750	562	9.2	9.8
17	875	875	500	750	600	789	875	500	750	600	37.2	37.6
18	350	525	425	750	600	435	495	401	750	600	14.0	14.6
19	350	875	500	750	600	475	830	500	750	600	24.0	24.4
20	525	875	500	750	600	780	830	500	750	600	34.5	34.8

suitable for on-line implementation of the capacitor control even for a very large distribution system. If a parallel computation scheme is used for the parallel neural networks, the response time of the control process would be further reduced. Additional off-line information obtained from the optimization techniques can be used to provide new training data for the expert system which will improve the accuracy of the optimal capacitor control.

The application of the proposed capacitor control will be mainly limited by the computation time required for the learning process which in turn depends on the number of conforming load groups and capacitors installed rather than the number of system buses. Considering the practically realistic number of conforming load groups and capacitors in the given example and the fact that the relatively time-consuming parameter computation is performed only in the learning stage, the applicability of the control technique to

distribution systems with many more buses than in the example seems to be promising.

5. GENERAL CONCLUSIONS

The high cost of generation and transmission facilities as well as energy production have led to the need of minimizing peak power demand and energy losses. Furthermore, developments in distribution automatization through the use of substation-based computer and feeder data acquisition systems allow the implementation of real-time control of Var compensators, which will result in a substantial reduction of the system losses.

The work presented in this dissertation deals mainly with the design and control of distribution system capacitors. A piecewise method for obtaining optimum sizes and tap settings of capacitors installed on a radial distribution system has been developed to solve the problem of large system size. The results of the proposed method can be implemented through a centralized substation computer, as a part of distribution automatization scheme, or by local controllers performing the capacitor switchings. The simulation results show the significance of proper load representation if the economic savings obtained by capacitor installation is used as a figure of merit for the capacitor design.

The capacitor control is provided by a neural-net based expert system featuring two stages of artificial neural network. From the direct measurements at certain buses as well as the current capacitor settings the first stage of the control network determines the load profile which is then used for finding the best capacitor settings in the next stage. This control algorithm is suitable for a centralized control scheme. Moreover, since it is computationally very efficient, it is suitable for on-line implementation even for a very large distribution system. The application of the proposed capacitor control will be mainly limited by the computation time required for the learning process which in turn depends on the number of conforming load groups and capacitors installed. Performance of the control network can be further improved by periodically retraining the control network with new

learning data as well as providing a parallel computation scheme.

The design and control algorithm can be modified to include voltage regulators, voltage constraints, unconventional Var compensators, harmonic effects and other practical considerations in the problem formulation for which further research is recommended.

REFERENCES

[1] S. Civanlar and J. J. Grainger, "Volt/Var control on distribution systems with lateral branches using shunt capacitors and voltage regulators: parts I, II & III", *IEEE Trans. Power Apparatus & Systems*, vol.104, pp. 3278-3297, Nov 1985.

[2] N. M. Neagle and D. R. Samson, "Loss reduction from capacitors installed on primary feeders", *AIEE Trans.*, vol. 75, part III, pp.950-959, Oct 1956.

[3] R. F. Cook, "Optimizing the application of shunt capacitors for reactive-volt-ampere control and loss reduction", *AIEE Trans.*, vol. 80, pp.430-444, Aug 1961.

[4] R. F. Cook, "Calculating loss reduction afforded by shunt capacitor application", *IEEE Trans. Power Apparatus & Systems*, vol. 83, pp.1227-1230, Dec 1964.

[5] N. E. Chang, "Locating shunt capacitors on primary feeder for voltage control and loss reduction", *IEEE Trans. Power Apparatus & Systems*, vol. 88, pp.1574-1577, Oct 1969.

[6] J. V. Schmill, "Optimum size and location of shunt capacitors on distribution feeders", *IEEE Trans. Power Apparatus & Systems*, vol. 84, pp.825-833, Sep 1965.

[7] H. Duran, "Optimum number, location and size of shunt capacitors in radial distribution feeders, a dynamic programming approach", *IEEE Trans. Power Apparatus & Systems*, vol. 87, pp. 1769-1774, Sep 1968.

[8] M. Ponnavaikko and K. S. Prakasa Rao, "Optimal choice of fixed and switched shunt capacitors on radial distribution feeders by the method of local variations", *IEEE Trans. Power Apparatus & Systems*, vol.102, pp. 1607-1615, June 1983.

[9] M. Kaplan, "Optimization of number, location, size, control type and control setting of shunt capacitors on radial distribution feeders", *IEEE Trans. Power Apparatus & Systems*, vol.103, pp. 2659-2665, Sept 1984.

[10] R. G. Rinker and D. L. Rembert, "Using the reactive current profile of a feeder to determine optimal capacitor placement", *IEEE Trans. Power Delivery*, vol.3, pp.411-416, Jan 1988.

[11] J. J. Grainger and S. H. Lee, "Optimum size and location of shunt capacitors for reduction of losses on distribution feeders", *IEEE Trans. Power Apparatus & Systems*, vol.100, pp.1105-1118, March 1981.

[12] J. J. Grainger and S. H. Lee, "Capacity release by shunt capacitor placement on distribution feeders: a new voltage-dependent model", *IEEE Trans. Power Apparatus & Systems*, vol.101, pp.1236-1244, May 1982.

[13] J. J. Grainger, S. Civanlar, K. N. Clinard and L. J. Gale, "Optimal voltage dependent continuous time control of reactive power on primary feeders", *IEEE Trans. Power Apparatus & Systems*, vol.103, pp. 2714-2722, Sept 1984.

[14] A. A. El-Kib, J. J. Grainger, K. N. Clinard and L. J. Gale, "Placement of fixed and/or non-simultaneously switched capacitors on unbalanced three-phase feeders involving laterals", *IEEE Trans. Power Apparatus & Systems*, vol.104, pp.3298-3305, Nov 1985.

[15] M. E. Baran and F. F. Wu, "Optimal capacitor placement on radial distribution systems", *IEEE Trans. Power Delivery*, vol 4, pp. 725-734, Jan 1989.

[16] M. E. Baran and F. F. Wu, "Optimal sizing of capacitors placed on a radial distribution system", *IEEE Trans. Power Delivery*, vol.4, pp. 735-743, Jan 1989.

[17] H. D. Chiang, J. C. Wang, O. Cockings and H. D. Shin, "Optimal capacitor placement in distribution systems: Part 1: A new formulation and the overall problem; Part 2: Solution algorithm and numerical results", *IEEE PES 1989 Summer Meeting*, Paper 89 SM 767-4,5, Long Beach, CA, July 9-14, 1989.

[18] H. H. Happ, "Diakoptics and Piecewise Methods", *IEEE Trans. Power Apparatus & System*, vol.89, pp. 1373-1382, Sep/Oct 1970.

[19] A. E. Emanuel, "Suggested definition on reactive power in nonsinusoidal systems", *Proc. Inst. Elec. Eng.*, vol.121, pp. 705-706, July 1974.

[20] G. G. Richards, O. T. Tan, P. Klinkachorn and N. I. Santoso, "Cost-constrained

power factor optimization with source harmonics using *LC* compensators", *IEEE Trans. Industrial Electronics*, vol.34, pp.266-270, May 1987.

[21] E. C. McClelland and P. R. Van Horne, "Fast voltage prediction using a knowledge based approach", *IEEE Trans. Power Apparatus & Systems*, vol. 102, pp. 315-319, Feb 1983.

[22] T. Sakaguchi and K. Matsumoto, "Development of a knowledge based system for power system restoration", *IEEE Trans. Power Apparatus & Systems*, vol. 102, pp.320-329, Feb 1983.

[23] C. C. Liu and K. Tomsovic, "An expert system assisting decision-making of reactive power/voltage control", *IEEE Trans. Power Systems*, vol. 1, pp.195-201, Aug 1986.

[24] S. J. Cheng, O. P. Malik, and G. S. Hope, "An expert system for voltage and reactive power control of a power system", *IEEE Trans. Power Systems*, vol. 3, pp. 1449-1455, Nov 1988.

[25] R. Fujiwara, T. Sakaguchi, Y. Kohno and H. Suzuki, "An intelligent load flow engine for power system planning", *IEEE Trans. Power Systems*, vol. 1, pp.302-307, Aug 1986.

[26] D. J. Sobajic and Y. H. Pao, "Artificial neural-net based dynamic security assessment for electric power systems", *IEEE Trans. Power Systems*, vol. 4, pp. 220-228, Feb 1989.

[27] S. Ebron, D. L. Lubkeman, M. White, "A neural network approach to the detection of incipient status on power distribution feeders", *IEEE PES Transmission and Distribution Conference*, New Orleans, LA, April 2-7, 1989.

[28] C. C. Liu, S. J. Lee, S. S. Venkata, "An expert system operational aid for restoration and loss reduction of distribution systems", *IEEE Trans. Power Systems*, vol. 3, pp. 619-626, May 1988.

[29] Scientific System, Inc., *Optimization of Reactive Volt-Ampere(VAR) Sources in System Planning, Vol.1:Solution Technique, Computing Methods, and Results*, EPRI EL-3729, vol.1, Project 2109-1, Nov 1984.

[30] J. B. Bunch, R. D. Miller and J. E. Wheeler, "Distribution system integrated voltage and reactive power control", *IEEE Trans. Power Apparatus & Systems*, vol. 101, pp. 284-289, Feb 1982.

[31] J. Qiu and S. M. Shahidehpour, "A new approach for minimizing power losses and improving voltage profile", *IEEE Trans. Power Systems*, vol. 2, pp. 287-295, May 1987.

[32] S. Civanlar, J. J. Grainger, H. Yin, S. S. H. Lee, "Distribution feeder reconfiguration for loss reduction", *IEEE Trans. Power Delivery*, vol.3, pp. 1217-1223, July 1988.

[33] M. E. Baran and F. F. Wu, "Network reconfiguration in distribution systems for loss reduction and load balancing", *IEEE Trans. Power Delivery*, vol.4, pp.1401-1407, April 1989.

[34] T. J. E. Miller, *Reactive Power Control in Electric Systems*, John Wiley & Sons, Inc., 1982.

[35] Turan Gonen, *Electric Power Distribution System Engineering*, MacGraw-Hill, Inc., 1986.

[36] T. Longland, T. W. Hunt, W. A. Brechnell and C. A. Worth, *Power Capacitor Handbook*, Butterworth & Co., 1984.

[37] S. S. Rao, *Optimization Theory and Applications*, John Wiley & Sons, 1984.

[38] R. F. Chu and R. H. Avendano, "A direct method for identifying the optimal power factor correction in nonsinusoidal systems", *IEEE Trans. Power Apparatus & Systems*, vol.104, pp. 959-964, April 1985.

[39] J. Arrillaga, D. A. Bradley and P. S. Bodger, *Power System Harmonics*, John Willey & Sons, Inc., 1985.

[40] M. F. McGranaghan, J. H. Shaw and R. E. Owen, "Measuring voltage and current harmonics on distribution systems", *IEEE Trans. Power Apparatus and Systems*, vol. 100, pp. 3599-3608, July 1981.

[41] T. Hiyama, M. S. A. A. Hamman and T. H. Ortmeyer, "Distribution system modeling with distributed harmonic sources", *IEEE Trans. on Power Delivery*, vol.4, pp. 1297-1304, April 1989.

[42] D. T. Rizy, E. W. Gunther, M. F. McGranahan, "Transient and harmonic voltages associated with automated capacitor switching on distribution systems", *IEEE Trans. Power Systems*, vol.2, pp. 713-723, Aug 1987.

[43] L. S. Czarnecki, "Minimization of distorted power of nonsinusoidal sources applied to linear loads", *Proc. Inst. Elec. Eng.*, vol.128, pt. C, pp. 208-210, July 1980.

[44] W. Shephard and P. Zakikhani, "Power factor correction in nonsinusoidal systems by the use of capacitance", *J. Phys. D: Appl. Phys.*, vol.6, pp. 1850-1861, 1973.

[45] L. S. Czarnecki, "Consideration on the reactive power in nonsinusoidal situations", *IEEE Trans. Instrumentation & Measurements*, vol. 34, pp. 399-404, Sept 1985.

[46] Y. Baghzouz and S. Ertem, "Shunt capacitors sizing for radial distribution feeders with distorted substation voltage" *IEEE PES 1989 Summer Meeting*, Paper 89 768-3, Long Beach, CA, July 9-4, 1989.

[47] R. K. Hartana and G. G. Richards, "Optimum filter design for distribution feeders with multiple harmonic sources", submitted to *IEEE Trans. Power Systems*.

[48] N. I. Santoso and O. T. Tan, "Optimal design of switchable distribution capacitors by piecewise method", *Archiv fur Elektrotechnik*, to appear.

[49] H. H. Happ, "Diakoptics - the solution of system problems by tearing", *Proc. IEEE*, vol.62, No.7, pp. 930-940, July 1974.

[50] H. H. Happ, *Piecewise Method and Applications to Power Systems*, Wiley-Interscience Publication, John Wiley, 1980.

[51] G. T. Heydt, *Computer Analysis Methods for Power Systems*, Macmillan Publishing Co., 1986.

[52] A. M. Geoffrion, "Generalized Benders Decomposition", *JOTA*, vol.10, pp. 237-260, April 1972.

[53] D.T. Rizy, J. S. Lawler, J. B. Patton and W. R. Nelson, "Measuring and analyzing the impact of voltage and capacitor control with high speed data aquisition", *IEEE Trans. Power Delivery*, vol. 4, pp. 704-714, Jan 1989.

[54] W. W. Price, K. A. Wirgau, A. Murdoch, J. V. Mitsche, E. Vaahedi and M. A. El-Kady, "Load modeling for power flow and transient stability computer studies", *IEEE Trans. Power Systems*, vol.3, pp. 180-187, Feb. 1988.

[55] N. I. Santoso and O. T. Tan, "Piecewise method for optimal sizing of distribution capacitors", *Proc. IASTED International Symposium on Simulation and Modelling*, Lugano, Switzerland, June 19-22, pp.107-110, 1989.

[56] E. Handschin and Ch. Bornemann, "Bus load modeling and forecasting", *IEEE Trans. Power Systems*, vol. 3, pp. 627-633, May 1988.

[57] T. R. Feldman, "Microprocessor-based controllers and an intelligent capacitor-bank controller", *IEEE Trans. Power Apparatus & Systems*, vol. 103, pp. 2780-2784, Sep 1984.

[58] N. I. Santoso and O. T. Tan, "Neural-net based real-time control of capacitors installed on distribution systems", *IEEE PES 1989 Summer Meeting*, Paper 89 SM 768-3, Long Beach, CA, July 9-14, 1989; to appear in *IEEE Trans. Power Delivery.*

[59] W. B. Gevarter, *Artificial Intelligence, Expert Systems, Computer Vision and Natural Language Processing,* Noyes Publications, 1984.

[60] W. B. Rauch-Hindin, *A Guide to Commercial Artificial Intelligence: Fundamentals and Real-World Applications,* Prentice Hall 1988.

[61] R. P. Lipmann, "An introduction to computing with neural nets" , in V. Vemuri (Ed.), *Artificial Neural Networks: Theoretical Concepts,* IEEE Computer Society Press, 1988.

[62] D. E. Rumelhart, G. E. Hinton and R. J. Williams, "Learning internal representations by error propagation", in D. E. Rumelhart and J. L. McClelland (Eds.), *Parallel Distributed Processing: Exploration in The Microstructure of Cognition, Vol.1: Foundations,* MIT Press, 1987.

[63] *IEEE Guide for Harmonic Control and Reactive Compensation of Static Power Converters*, IEEE Standard 519-1981, 1981.

Appendix A. VAR SOURCE APPLICATION GUIDE [29]

System Problem	*Typical Var Compensation*	*Speed of response*
Low voltages*	Fixed shunt capacitors	
High voltages*	Shunt reactors	
Large voltage variability*	Fixed shunt capacitors/reactors, synchronous condensers	
Excessive reactive power flows*	Fixed shunt capacitors	
Normal reactive requirements for HVDC converters*	Fixed shunt capacitors	
Steady-state stability*	Fixed shunt and series capacitors	
Fluctuating reactive loads or impact loads**	Synchronous condensers, SVC	slower
Switching surges or load rejection overvoltages**	Shunt reactors, SVC	
Voltage instability**	Fixed shunt capacitors with SVC or synchronous condensers	
Transient and dynamic stability**	Series capacitors, SVC, Synchronous condensers	
Instability due to subsysnchonous resonance**	SVC	
Variable system phase imbalances	SVC	
Dynamic reactive requirements at HVDC terminals**	Fixed shunt capacitors and SVC	faster

* Steady-state system problem

** Dynamic system problem

Appendix B. COST-CONSTRAINED POWER FACTOR OPTIMIZATION WITH SOURCE HARMONICS USING AN *LC* COMPENSATOR

A method is presented for finding the optimum *LC* combination for power factor compensation at linear loads in the presence of voltage source harmonics while the total voltamperes of the compensator capacitor and reactor is constrained [20].

B.1. Objective Function and Cost Constraint

A single-phase network equivalent of the system considered is shown in Fig. B.1, where the Thevenin nonsinusoidal source voltage is represented by

$$v_s(t) = \sum_n v_{sn}(t) \tag{B.1}$$

in which n is the order of harmonic present. The Thevenin source impedance for the nth harmonic is

$$Z_{tn} = R_{tn} + jX_{tn} \tag{B.2}$$

and the nth harmonic equivalent impedance of the linear load is represented by

$$Z_{ln} = R_{ln} + jX_{ln} \tag{B.3}$$

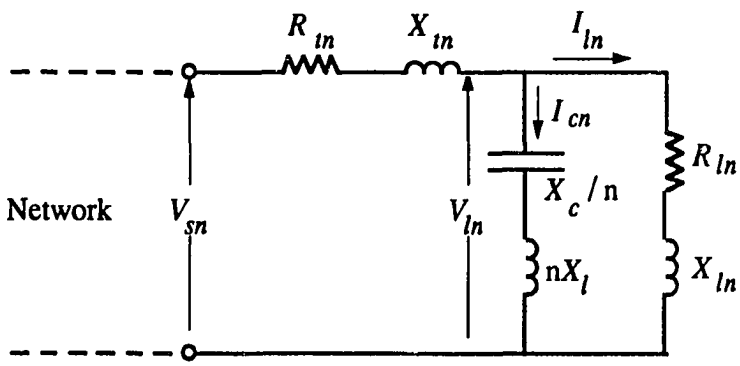

Fig. B.1. System model

The rms line current squared is

$$I_s^2 = \sum_n I_{sn}^2 \tag{B.4}$$

with

$$I_{sn} = V_{sn}/Z_n \tag{B.5}$$

in which Z_n is the impedance seen from the Thevenin source for the nth harmonic frequency, and given by

$$Z_n = R_{tn} + jX_{tn} + \frac{j(R_{ln} + jX_{ln})(nX_L - X_C/n)}{R_{ln} + j(X_{ln} + nX_L) - X_C/n}. \tag{B.6}$$

In (B.6), $X_L = \omega_0 L$, and $X_C = 1/\omega_0 C$, where ω_0 is the fundamental frequency.

The LC compensator has to be selected so as to maximize the compensated load power factor, which is defined as

$$PF = \frac{\sum_n V_{ln} I_{sn} \cos(\angle V_{ln} - \angle I_{sn})}{V_l I_s} \tag{B.7}$$

where

$$V_l = \left[\sum_n V_{ln}^2\right]^{1/2} \tag{B.8}$$

From (B.7) it follows that power factor maximization approximately corresponds to minimizing the rms line current which is explicitly dependent on X_C and X_L, and is chosen as the objective function in the optimization process. However, optimizing the objective function with respect to both X_C and X_L may not provide an economical solution, even if such a solution exists. Consequently, optimization of the objective function will be constrained by holding the total voltamperes of the compensator capacitor and reactor, corresponding to approximately the compensator cost, constant.

For capacitors and reactors, voltampere ratings are defined as [57]

$$S_C = \left[\sum_n I_{cn} X_C / \mathrm{n}\right]\left[\sum_n I_{cn}^2\right]^{1/2} \quad \text{kVA} \tag{B.9}$$

and

$$S_L = \left[\sum_n I_{cn} \mathrm{n}\, X_L\right]\left[\sum_n I_{cn}^2\right]^{1/2} \quad \text{kVA} \tag{B.10}$$

where the compensator current I_{cn} is related to I_{sn} by

$$I_{cn} = \frac{R_{\mathrm{ln}} + j\, X_{\mathrm{ln}}}{R_{\mathrm{ln}} + j\,(X_{\mathrm{ln}} + \mathrm{n}\, X_L - X_C/\mathrm{n})}\, I_{sn}. \tag{B.11}$$

In (B.9) and (B.10), the harmonic voltages are added linearly in the first summation to emphasize the effect of peak (as opposed to rms) voltage or insulation cost. The variable part of the compensator cost is then

$$K = U_C S_C + U_L S_L \tag{B.12}$$

where U_C and U_L are respectively the costs of capacitor and inductor per kVA and considered to be constant parameters.

Equation (B.12), along with (B.9), (B.10), and (B.11), represents the constraint for the minimization of objective function (B.4). Thus the values of X_C and X_L have to be chosen such that expression (B.4) is minimized and (B.12) is simultaneously satisfied for any given cost K.

B.2. Optimization Algorithm

Equation (B.12) is an implicit function of X_C and X_L , and cannot be solved explicitly for X_C and X_L for substitution in the objective function (B.4) to convert the constrained problem into an unconstrained minimization of I_s^2 . However, the

optimization problem can be solved by the Lagrangian multiplier method by writing the constraint (B.12) as

$$g(X_C, X_L) = U_C S_C + U_L S_L - K = 0 \tag{B.13}$$

Then the Lagrange function is

$$£(X_C, X_L, \lambda) = I_s^2 + \lambda\ g(X_C, X_L) \tag{B.14}$$

where λ is the Langrange multiplier. The minimum of the unconstrained function £ is found by

$$\frac{\partial £}{\partial X_C} = \frac{\partial I_s^2}{\partial X_C} + \lambda \frac{\partial g}{\partial X_C} = 0, \tag{B.15}$$

$$\frac{\partial £}{\partial X_L} = \frac{\partial I_s^2}{\partial X_L} + \lambda \frac{\partial g}{\partial X_L} = 0, \tag{B.16}$$

$$\frac{\partial £}{\partial \lambda} = g(X_C, X_L) = 0. \tag{B.17}$$

Elimination of λ from (B.17) and (B.18) results in

$$\frac{\partial I_s^2}{\partial X_C} - \frac{\partial I_s^2}{\partial X_L}\left[\frac{\partial g}{\partial X_C} / \frac{\partial g}{\partial X_L}\right] = 0 \tag{B.18}$$

or

$$\frac{\partial I_s^2}{\partial X_L} - \frac{\partial I_s^2}{\partial X_C}\left[\frac{\partial g}{\partial X_L} / \frac{\partial g}{\partial X_C}\right] = 0. \tag{B.19}$$

Every set of values for X_C and X_L maximizing the power factor will satisfy (B.18) and (B.19) at a cost which can be computed by (B.17) or (B.12).

The solutions to (B.17) and (B.18) or (B.19) will be obtained with an optimization algorithm based on the reduced gradient technique which will locate maximum power factors by searching along the constant-cost power factor ridges, shown in Fig. 2.5, for the

point where the gradient of I_s^2 (and thus power factor) is zero. Note that each zone in the X_C -X_L plane will generally contain a family of constant-cost power factor ridges. Therefore, each of the zones must be searched for a maximum power factor for any given cost, which is then to be compared with the maximum power factors for the same cost in the other zones.

The algorithm proceeds as follows. A number of compensator costs are preselected to range from zero to approximately twice the cost of only compensating the load fundamental reactive voltamperes. Next, X_C is fixed to be above the highest series-resonance value for $X_L = 0$, and X_L is searched until each of the preselected costs in each of the zones is approximately encountered. This initializes X_C and X_L for the iterative optimization process. Then, taking X_C as the control variable and X_L as the dependent variable, the algorithm increments X_C in the direction of decreasing I_s^2 along the constant-cost curve by

$$\Delta X_C = \alpha\left\{\frac{\partial I_s^2}{\partial X_C} - \frac{\partial I_s^2}{\partial X_L}\left[\frac{\partial g}{\partial X_C}/\frac{\partial g}{\partial X_L}\right]\right\} \tag{B.20}$$

where α is a scalar to control the magnitude of the X_C increment. X_L is then incremented by an amount ΔX_L such that the cost given in (B.12) is constant:

$$\Delta X_L = -\left[\frac{\partial g}{\partial X_C}/\frac{\partial g}{\partial X_L}\right]\Delta X_C \tag{B.21}$$

To keep the step size sufficiently small in order to maintain the cost constant during the search, it is necessary to limit expression (B.21). If

$$\left|\frac{\partial g}{\partial X_C}/\frac{\partial g}{\partial X_L}\right| > 1 \tag{B.22}$$

then the X_C and X_L variables are reversed in computation role by taking X_L as the control variable:

$$\Delta X_L = \alpha\left\{\frac{\partial I_s^2}{\partial X_L} - \frac{\partial I_s^2}{\partial X_C}\left[\frac{\partial g}{\partial X_L}/\frac{\partial g}{\partial X_C}\right]\right\} \tag{B.23}$$

and X_C as the dependent variable:

$$\Delta X_C = -\left[\frac{\partial g}{\partial X_L}/\frac{\partial g}{\partial X_C}\right]\Delta X_L \tag{B.24}$$

Similarly, if

$$\left|\frac{\partial g}{\partial X_L}/\frac{\partial g}{\partial X_C}\right| \geq 1 \tag{B.25}$$

equations (B.20) and (B.21) should be used.

In accordance with (B.18) and (B.19), the optimum point is obtained when the gradient of I_s^2 relative to X_C and X_L is zero. Therefore, the iterative search is terminated when $|\Delta X_C| + |\Delta X_L|$ is sufficiently small. The power factor and compensator cost are then computed and recorded, X_C is returned to its original value and the next initial value for X_L is located. The process repeats until the power factor maxima are found for a sufficient number of costs in each of the zones. Then, the pairs of values of power factor and cost generated are ranked to eliminate the inferior zonal maxima and plotted as a single power factor curve against compensator cost or capacitor and reactor ratings. The optimization procedure is illustrated by the flowchart in Fig. B.2.

B.3. Remarks

LC compensators for improving power factor of linear loads with source harmonics have been investigated. It is shown that, although a proper optimum power factor not constrained by compensator cost may not exist, a maximum power factor does exist if the cost constraint is introduced. This maximum power factor plotted against compensator cost can be used to select the compensation level for a given load.

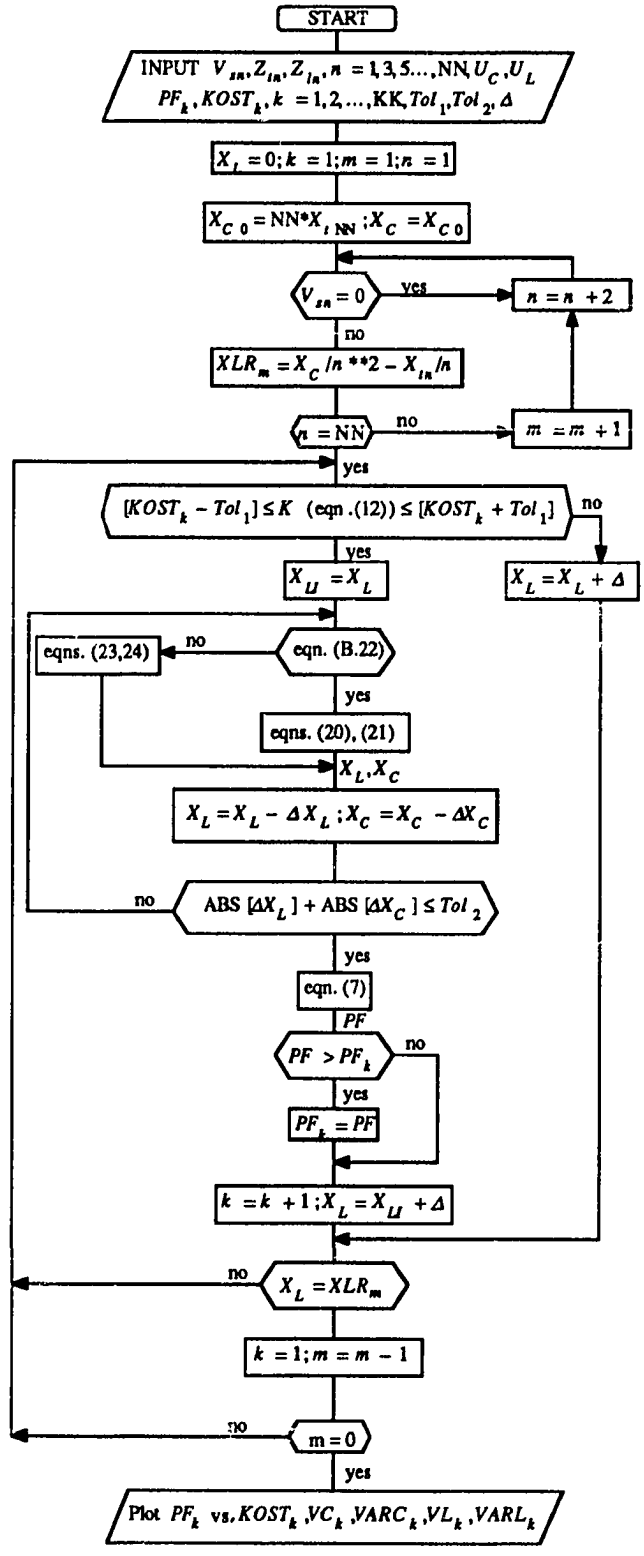

Fig. B.2. Optimization procedure

The relationship between maximum power factor and compensator cost is monotonically increasing, and in the examples appears almost linear for power factor values below 0.9. Since the incremental cost for power factor improvement remains constant in the linear part of the curve, an optimal economic compensation level may lie at the knee of the saturating power factor curve, where the incremental cost starts to rise offsetting the incremental tariff savings. However, the choice of compensation level will also be affected by local discount policies and varying load conditions.

The results also show that *LC* compensators can achieve a higher power factor than pure capacitive compensation for most loads when source harmonics are present. Conversely, the *LC* combination may provide a higher power factor than a pure capacitance of the same cost, even in cases where the unit cost of reactors is higher than that of capacitors.

In practice, the system parameter data may be uncertain. However, the proposed method may still be applied by finding the power factor curves for a variety of system conditions commensurate with those normally encountered, and selecting the capacitor and reactor for the best average performance.

VITA

N. Iwan Santoso was born on February 12, 1960, in Jakarta, Indonesia. He attended elementary school in Jakarta, and graduated from Canisius College High School in 1975. From 1976 to 1982, he worked on his Engineer degree at Trisakti University, Jakarta, Indonesia, while holding teaching assistantships and a part-time job. He continued his study at Louisiana State University and obtained his M.S. degree in Electrical Engineering in 1983. In January 1984, he started his Ph.D. program and since then has been holding a research assistantship in the Department of Electrical and Computer Engineering, LSU. Presently, he is a candidate for the degree of Doctor of Philosophy in Electrical Engineering.

DOCTORAL EXAMINATION AND DISSERTATION REPORT

Candidate: Nugroho Iwan Santoso

Major Field: Electrical Engineering

Title of Dissertation: Optimal Design and Control of Distribution System Capacitors

Approved:

Major Professor and Chairman

Dean of the Graduate School

EXAMINING COMMITTEE:

Date of Examination:

October 4, 1989